Stellenbosch
UNIVERSITY
IYUNIVESITHI
UNIVERSITEIT

The Design of a PocketQube Satellite Communication System

Gary Allen
23905093

October 24, 2023

UNIVERSITEIT·STELLENBOSCH·UNIVERSITY
jou kennisvennoot • your knowledge partner

Plagiaatverklaring / *Plagiarism Declaration*

1. Plagiaat is die oorneem en gebruik van die idees, materiaal en ander intellektuele eiendom van ander persone asof dit jou eie werk is.
   Plagiarism is the use of ideas, material and other intellectual property of another's work and to present is as my own.

2. Ek erken dat die pleeg van plagiaat 'n strafbare oortreding is aangesien dit 'n vorm van diefstal is.
   I agree that plagiarism is a punishable offence because it constitutes theft.

3. Ek verstaan ook dat direkte vertalings plagiaat is.
   I also understand that direct translations are plagiarism.

4. Dienooreenkomstig is alle aanhalings en bydraes vanuit enige bron (ingesluit die internet) volledig verwys (erken). Ek erken dat die woordelikse aanhaal van teks sonder aanhalingstekens (selfs al word die bron volledig erken) plagiaat is.
   Accordingly all quotations and contributions from any source whatsoever (including the internet) have been cited fully. I understand that the reproduction of text without quotation marks (even when the source is cited) is plagiarism

5. Ek verklaar dat die werk in hierdie skryfstuk vervat, behalwe waar anders aangedui, my eie oorspronklike werk is en dat ek dit nie vantevore in die geheel of gedeeltelik ingehandig het vir bepunting in hierdie module/werkstuk of 'n ander module/werkstuk nie.
   I declare that the work contained in this assignment, except where otherwise stated, is my original work and that I have not previously (in its entirety or in part) submitted it for grading in this module/assignment or another module/assignment.

Studentenommer / *Student number*	Handtekening / *Signature*
Voorletters en van / *Initials and surname*	Datum / *Date*

Contents

List of Figures

List of Tables

Nomenclature

Variables and functions

V	Voltage
I	Current
R	Resistance

Acronyms and abbreviations

GS	Ground Station
PQ	PocketQube
LEO	Low Earth Orbit
LOS	Line-of-Sight
PCB	Printed Circuit Board
EPS	Energy Power System
TX	Transmit
RX	Receive
GPS	Global Positioning System
GNNS	Global Navigation Satellite System
IMU	Inertial Measurement Unit
SU	Stellenbosch University
PQSU	PocketQube Stellenbosch University
RF	Radio Frequency
IC	Integrated Circuit
PEC	Perfect Electrical Conductor
ASK	Amplitude Shift Keying
PSK	Phase Shift Keying
FSK	Frequency Shift Keying
QAM	Quadrature Amplitude Modulation
GFSK	Gaussian Frequency Shift Keying
GUI	Graphical User Application
EIRP	Equivalent isotropic radiated power
UML	Unified modeling language
SF	Spreading factor
CSP	CubeSat Space Protocol
CCSDS	Consultative Committee for Space Data Systems
CRC	Cyclic Redundancy Check

Abstract

English

This report documents the design and implementation of a wireless communication system for a miniaturised satellite called a *PocketQube*. The PocketQube standard is a set of specifications which aim to make it easier for people to design small satellite modules that can easily integrate with each other. The standard is relatively new, however, and few designs have been published for a PocketQube communication system.

The design in this project includes both a tracking ground station, as well as a PocketQube module. The LoRa-based ground station was designed to mechanically track the satellite system using a pre-defined GPS path, as well as wirelessly recieved GPS data. The system was then implemented, and the communication link was tested up to 50 km line-of-sight and found to be reliable at a baud rate of 9600 bps. The GPS tracking was also tested and proved to be a robust method. Finally, the ground station was tested with data received from a third party radiosonde as a backup using a software-defined radio. This report documents the design choices and constraints, analyses the results of the system, and suggests improvements for future projects.

1. Introduction

1.1 Overview

This project aims to design and implement a wireless communication system for a miniaturised satellite standard called a *PocketQube* (PQ). The PocketQube standard was created to define physical and electronic requirements for so-called ”nano satellites”. The goal of this is to allow for easy integration of various sub-modules into one physical enclosure. One common use-case of these satellites is to collect sensory information from the atmosphere.

Nano-satellites can either be placed into orbit, or attached to a *high-altitude balloon* as shown in Figure 1.1. The goal of this project is to design a communication system that is compatible with the PocketQube standard. The final system should be capable of being used in a balloon satellite launch from the Saldanha Air Field in the Western Cape, which might be done by the Stellenbosch Engineering department near the end of the project.

Figure 1.1: A Balloon Satellite

Both higher-level systems design, as well as more detailed lower-level component selection, integration, and software design, will be necessary for this project. The communication system will involve both a tracking ground station (GS), as well as a PocketQube 'unit' (PQU). The aim of this project is to both design and implement this system, in order to establish a minimal baseline for further projects to refine the individual sub-systems. The GS should also be capable of receiving information from an existing *Radiosonde* to provide a backup system.

In this report, general system requirements are first listed, and a problem statement is drawn up. Then, a literature review is conducted to gather background information in the fields of interest. This includes an overview of the PocketQube standard, antenna theory, satellite tracking, telecommunication theory, and PCB design. A system's level design is then done, which is followed by a more detailed design. Finally, the system is implemented and tested, and the results are discussed, as well as potential improvements for future projects.

1.2 Problem Statement

The initial problem statement provided was simply to design a communication system for a PocketQube, with focus on the ground station. As this statement is relatively broad, further investigation is necessary to clearly defined the problem. The requirements for this project are therefore defined by analysing general, currently existing balloon-satellite systems, as well as taking into account the planned launch that this specific PocketQube is planned to be used in, as shown in Figure 1.2. Further, the existing radiosonde (an iMet-54 atmospheric telemetry device) is used as a reference, both for the new system's requirements and as a consideration for system integration.

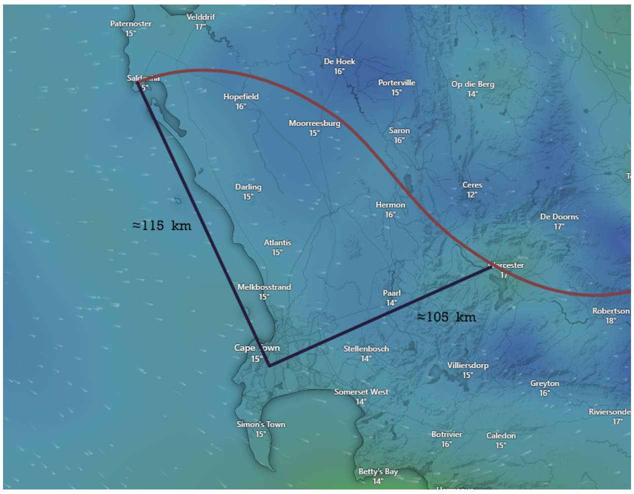

Figure 1.2: Planned Balloon Path and Distances

Generally, high-altitude balloons can drift to a height as much as 30 km above sea level [8]. For this project, the balloon is planned to be released from near Saldanha Bay, where it will travel a maximum distance of around 200 km towards the Cederberg, and land furthest in Worcester. From Cape Town, this is a maximum straight line distance of around 115 km.

The GS should maintain a reliable wireless link with the PQU to enable continuous communication. Realtime data transmission and telemetry should be maintained. Since most radiosondes are simply uni-directional "downlink" devices, this should be a priority requirement, however the system should also be capable of simple bi-directional communication.

An existing two-axis antenna mount has been provided by the Stellenbosch department. If this is to be used, the integration of a custom PCB design onto this mount should be done for the GS. Lastly, the PQ unit should also conform to the PQ standard, and fit inside a provided housing.

1.3 Requirements

As mentioned, the general requirement of this system is that continuous, wireless communication should be established and maintained between the ground station and a balloon-satellite carrying a PocketQube payload. From this information, and after supervisor consultation, slightly more specific user requirements are gathered and listed:

1. The GS should be capable of receiving data continuously and wirelessly from the PQ, as well as data from the priorietary Radiosonde.

2. The communication system should be capable of the range covered in Figure 1.2.

3. The PQ unit should conform to the *SU-modified* PQ9 standard (listed in Appendix C.1), and integrate with other prototype units. This standard is here-on refered to as *PQSU*.

4. The PQ unit should remain operational for ”a few hours”.

5. The GS electronics should integrate into an existing antenna mount.

The system will undergo a *flight-readiness review* to determine if it has met the requirements before launch. These requirements mostly include the neccessity to monitor the satellite from take-off and for an hour thereafter, and in that case the full 110 km range would not be required as the ground station could theoretically be placed closer. However, the system should be designed for this range, in order to cater for the full flight path. Further, as the project progresses, if supporting greater distances (200+ km) will not significantly increase the time, complexity, or cost of the system, it could be catered for as an expansion to the core requirements. It should be noted, however, that the nature of this project (a system's level design) means that such optimizations should not be made a priority.

1.4 Specifications

For specification definition, further calculations should be done. This will allow a list of more detailed, system-level specifications to be created. First, the required communication conditions (link distance, atmospheric effects etc.) are established. Then, power and voltage requirements are expanded on. Finally, system integration is considered.

Typicall balloon satellites reach a maximum height of around 30 km [8]. They rise at a vertical speed of around 20 km/h, and can travel horizontally as fast as 200 km/h when falling. A typical path distance for such a balloon is 200 km, and therefore an average speed of around 100 km/h will be designed for. This results in an average flight time of longer than 2 hours.

At the above height, a line-of-sight (LOS) calculator reveals that the horizon is around 600 km, meaning that the antenna could theoretically be placed at sea level, assuming no ground obstructions. Further, the earth's curvature is found to be negligible at this distance, meaning pythagoras can be used to calculate a final LOS distance of 120 km. If low-earth orbit (LEO) heights are to be considered as a project expansion, the curvature of the earth should be taken into account. At a height of 160 km, an LOS distance of 1400 km is required, and at 1000 km, an LOS distance of around 3500 km is required. Since this is much further than the required slant range of 120 km, it will not be designed for initially.

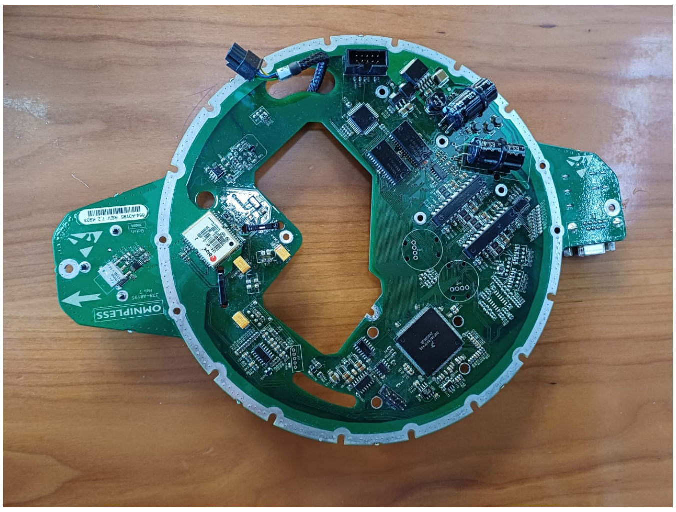

Figure 1.3: Existing Antenna Mount PCB

The PQSU standard includes 3.3V and 5V bus voltages. One of these must therefore be used directly to power the PQ unit's circuitry. As mentioned, the PQ unit will be integrated with other units into a single PocketQube. Since this is a prototype launch, there is risk of the EPS malfunctioning. Further, a power connection is also needed during development for modularized testing. A simple on-board battery system which matches the standard's voltage will therefore be included in the design to be used for testing and potentially deployment.

The PQSU standard clearly defines the dimensions of a PocketQube PCB (e.g. 42 mm x 42 mm outer dimensions) and the design should conform to this standard. The provided antenna mount allows for an existing circular PCB with mounting holes and two support "wings", as shown in 1.3. The new GS PCB should therefore conform to this form factor. Lastly, the system should drive the stepper motors which are already provided with the antenna mount. The following system-level specifications are therefore drawn up:

1. The system should be capable of a slant range of 120 km.

2. The system should be designed to operate at a minimum data rate of 4800 baud (which the iMet-54 uses [9]) or at a target data rate of 9600 baud (which is a typical satellite telemetry downlink speed as in [10]).

3. The system should allow for iMet-54 radiosonde data to be retreived. This data is GFSK modulated at a pre-selected frequency of between 402 to 405 MHz [9].

4. A single antenna should be used for both the custom and radiosonde protocol on the GS, to simplify the design. This antenna should therefore have a bandwidth in the range from 405 MHz up to the amateur radio band (433 MHz).

5. A 100 mW equivalent transmit power restriction should be adhered to.

6. The PQ unit should follow the PQSU and PQ9 standard, which stipulate:

   - A 42 mm square outer PCB dimension
   - A 4 mm component height above, and a 2 mm component height below.
   - A 20-pin header interface, catering for RS-485 and I2C communication, and providing 3.3 V and 5 V power lines.

7. The PQ unit should include a battery capable of lasting 2 hours at nominal current draw.

8. The GS should be capable of tracking the balloon at 110 km/h, at a line-of-sight distance of 120 km.

9. The GS PCB should connect to the existing antenna mount, which has a diameter of 198 mm, with equi-spaced mounting holes etc. (as in Figure 1.3).

10. The GS should control two 4218S-15 bipolar stepper motors, which have a maximum current of 0.50 A per phase, and are driven at 24 V.

11. The GS should provide a USB-C connection to allow a PC to monitor the telemetry data. This should be capable of receiving all data from the link in realtime.

2. Background

2.1 PocketQube

The PocketQube standard is a fairly new set of protocols and specifications defining a modularized nano-satellite system. The term *modularized* in this context refers to the ability for different ”modules” or PocketQube units, each with their own set functionality, to be connected to a common *backplane* and integrated seamlessly. *Integration* here refers to both the mechanical spacing of each module, as well as the electronic communication between the modules.

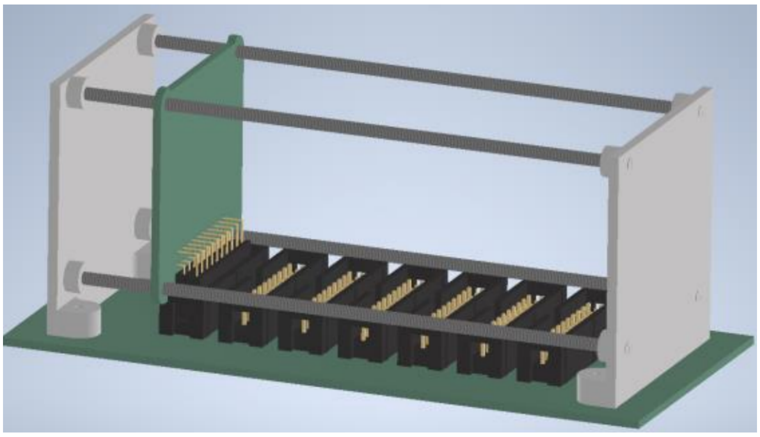

Figure 2.1: A PQSU Enclosure [1]

As an example, a PocketQube enclosure could contain three units: a communication module, a sensor pack, and a battery system. These modules can then be connected onto the backplane via headers, and placed inside a single enclosure, such as that in Figure 2.1. This ”nano-satellite” can then be ”launched” through any means.

2.2 Satellite Tracking

There are various methods used to track satellites in order to keep maintain communication. Ultimately, all of these methods provide a single output to a ground station system: the direction in which to ”steer” its antenna. Each method is compared and expanded on below.

2.2.1 Open-Loop

Arguably the simplest method is using what may be referred to as ”open-loop” control. In this method, information about the flight path of the balloon is fed into the system, such as expected GPS co-ordinates at different points in time, and the ground station is simply pointed in that direction, with the ”hopes” of maintaining a connection. The flight path can either be a pre-calculated path, or be continuously re-estimated based on realtime weather data. *Habhub* is an online high-altitude path predictor [11] which is freely available.

An advantage of this method is its extreme simplicity to implement. It has several disadvantages, however, including being vulnerable to prediction inaccuracies, as well as the difficulty experienced in re-acquiring the communication link once it is lost. Further, a GPS receiver is generally still required on the ground station, unless it is placed in a pre-determined location.

2.2.2 GPS (Direct)

If an initial communication link can be estabilished between the satellite and ground station, *direct* GPS transmission can be added for positional feedback. This is a simple method of ”closing” the tracking loop, since the path data can be updated dynamically.

Generally, both the PQ and GS GPS co-ordinates are required. Once these are retrieved, the GPS co-ordinates (known as the *WGS84* system) can be *projected* to a cartesian system using *Mercator projection* [12].

2.2.3 GPS (Relay)

If a link cannot be initially estabilished, a ”relay” method of GPS tracking can be used. This method functions in a three-step process, explained below and depicted in Figure 2.2:

1. The precise position of the payload and the ground station is determined using data received from GPS satellites.
2. The position is *relayed* to an external network (satellite or ground -based) using a radio transmitter.
3. The ground station receives the location from the external network (e.g. via the internet).

The major disadvantage of this method is the additional cost required. Since an antenna capable of communicating with one of the external networks is required, two antennas are needed if direct communication with a ground station is desired (however this is usually no longer necessary as the relay network can be used). Further, the cost of subscribing to an external network is generally high.

This type of tracking works well if the satellite is physically close to the external network satellites, or if the ground station does not need to communicate in realtime, but merely needs access to location of the satellite (e.g. in a homemade cellphone balloon satellite launch).

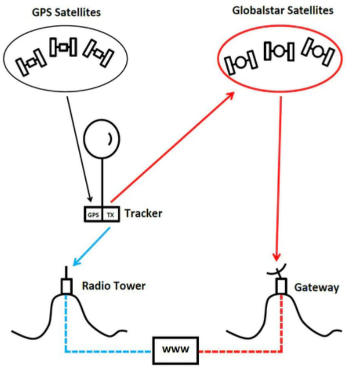

Figure 2.2: GPS Relay Tracking [2]

2.2.4 Signal Strength

Radio tracking can be done when the satellite itself transmits omni-directionally. The signal strength can then be used as feedback to determine the direction to point. To initially find the satellite, the entire sky can be scanned using a "brute force" procedure, or an initial guess can be provided. Then, periodic *radius scanning* can be used to track the signal within a certain portion of the sky, or more advanced techniques such as *conical scanning* can be used.

2.3 Antennas

This section covers a very brief review of different types of antennas in literature, as well as how to practical feed these antennas with a transmission line, and a summary of their varying performances.

2.3.1 Types

There are various antenna types to consider for a satellite communication system. A highly-customized antenna design is out of the scope of this project, and therefore only common designs with tunable parameters, or existing designs in literature, will be considered. Ultimately, the following characteristics will be used to compare the various options:

- Radiation pattern (qualitative shape)
- Gain (relative to an *isotropic* source)
- Bandwidth (relative to resonant frequency)
- Beamwidth (angular width of *main lobe*)
- Dimensions

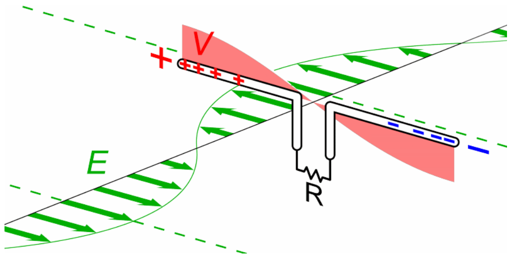

Figure 2.3: Dipole Antenna Illustration [3]

Half-Wavelength Dipole

The half-wavelength (0.5λ) dipole anntenna is arguably the simplest and most common type of antenna. It consists of two conductive elements operating in opposite phase, as depicted in Figure 2.3. It is considered *omni-directional* i.e. it radiates equally in a given plane. These antennas have a relatively low gain of around 2.15 dBi [7]. Further, they do not radiate in the direction tangential to their conductor.

General Dipole

Dipole antennas can, in general, be any length. However, a change in length results in a change in the antenna's characteristics. In general, smaller antennas result in lower gain and lower efficiency, but a larger beamwidth at the resonant frequency. The obvious advantage of these designs is that the size of the dipole can be decreased. However, if size is a constraint, *monopole* antennas are generally employed.

Quarter-Wave Monopole

The working principle of a classic monopole antenna makes use of the electromagnetic theory of *imaging*. If an infinite ground plane or Perfect Electrical Conductor (PEC) is placed below one half of a 0.5λ dipole antenna, then, since the PEC holds the constraint that the tangential electric field is zero across its boundary, an equal but opposite electromagnetic wave is "induced" due to the incident wave. This wave "appears" to have come from an equal but oppositely polarized "image" source, hence removing the need for the second half of the dipole to be present.

These antennas are extremely useful when size is a constraint, however have the disadvantage of requiring a ground plane. A *whip* antenna is a form of monopole antenna designed to be flexible so that it does not break as easily, and is often placed inside a plastic enclosure, as in Figure 2.4. [7]

Helical

Helical antennas are coiled windings of wire, where the circumference of the coil has some relationship with the desired wavelength. Commonly, a circumference of $C = 1.0\lambda$ is used for *unidirectional* variants. In this case, a ground plane is required (referring to the theory of

Figure 2.4: Whip Antenna in Plastic Housing

Figure 2.5: Helical, Unidirectional Antenna

imaging in Section 2.3.1). The ground plane can also be *cupped* (i.e. extended as an open cylinder) for additional directivity [13]. *Omni-directional* variants are also possible, which have a circumference much smaller than the operating wavelength, and do not require a ground plane [14]. When $C \approx \lambda$, the antenna is said to be operating in *axial mode*. Conversely, when $C << \lambda$, the antenna operates in *normal mode*. Figure 2.5 depicts a 21-turn antenna designed to operate in normal mode.

Helical antennas have several design parameters that influence the antennas characteristics, such as number of turns (n), wire width (wd), and spacing between turns (S). A spacing of $0.20\lambda < S < 0.25\lambda$ is recommended, however smaller spacings of $0.10\lambda < S < 0.20$ are commonly used [15]. They also are able to receive either linear or circularly polarized signals, making them more flexible. Lastly, since they can be designed with an arbitrarily small or large number of turns, and they have a large operating bandwidth, they can be made smaller than other alternatives.

Patch

A *patch* antenna (collequially known as a *PCB* antenna) is simply a rectangular PCB trace sized correctly to allow for radiation. Typically, a simple square or rectangular shape can be used. They allow for small profiles at the cost of efficiency [7], and can be integrated onto a PCB using normal trace techniques.

Array

In general, multiple antennas can be combined in what is known as an *array* configuration. This allows complete manipulation of the design, by virtue of *constructive* and *destructive* interference of the electromagnetic waves. This can allow for either an increase, or decrease in directivity. Common variations of this concept reside in *Yagi-Uda* and *Patch Array* antennas. [7]

Yagi-Uda

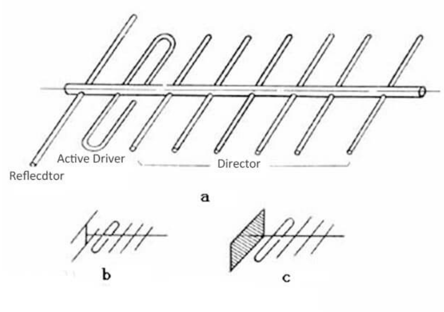

Figure 2.6: Yagi-Uda Antenna [4]

Although not strictly an antenna array, *Yagi-Uda* antennas are one of the most popular directive antennas. A given number of conductors are stacked in a specific configuration as show in Figure 2.6. This ultimately ”steers” the electromagnetic waves using the concept of interference. Only one of the conductors in the array is actually fed with the signal - the rest are merely *passive* elements used for increasing the directivity.

Microstrip

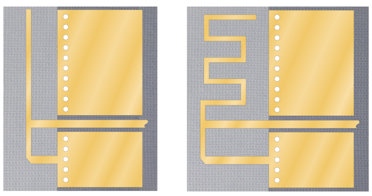

Figure 2.7: Inverted-F Microstrip Antennas [5]

Microstrip antennas generally refer to any planar, PCB antenna. They can be considered a generalization of a patch antenna. Many designs exist (often derived from non-planar antennas) due to their flexible nature. This allows for a diverse selection of desired characteristics. A few examples include:

- A *patch array*, which has increased directivity.
- An *inverted-F* design, which has a small form factorer and a nearly 3D omni-directional radiation pattern.

- A *ring antenna*, which is unidirectional, and has an even smaller form factor than the inverted-F antenna [16].
- A *helical patch* antenna, which is simply a "zig-zag" helix shape flattened onto a PCB.

A multi-frequency inverted-F design is illustrated in Figure 2.7.

2.3.2 Feedlines

In general, *feeding* an antenna is more complicated than simply connecting the amplifier's positive and negative terminals to the antenna's terminals. A $50\,\Omega$ characteristic impedance is often used in RF systems. Since each antenna has a unique *input impedance* which is generally different from this value, it must be *matched* appropriately for optimal performance.

A general, antenna-agnostic narrow-band technique for antenna impedance matching is to employ a "lumped element" matching circuit consisting mainly of inductors and capacitors. The most common example of this is an L-section, with exactly one capacitor and inductor. A few well-known techniques for a number of the antennas in Section 2.3.1 are reviewed below.

Half-Wavelength Dipole

A half-wavelength dipole antenna has an input impedance of around 73 ohms, varying only due to the wire diameter used. A common method to reduce this impedance to 50 ohms is simply to reduce the length of the dipole. In this case, a 50 ohms match occurs at between $0.42\,\lambda$ and $0.44\,\lambda$. [13]

Helical

The input impedance of a helical antenna varies between 100 and 200 ohms. A common method to reduce this impedance is for the first quarter turn of the helix to be in the form of a conductive strip, and for the *pitch angle* of this section to be close to zero [13]. The height above the ground plane can then be varied to match the antenna appropriately, with the following equation approximately providing an approximate $50\,\Omega$ match [13]:

$$h = \frac{w}{\frac{377}{\sqrt{\epsilon_r} Z_0} - 2}$$

2.3.3 Summary

The following table presents a general summary of the investigated antennas. A qualitative comparison of the results have been presented (from general consensus in literature) to aid in the design phase. Note that a *narrow* beamwidth general corresponds to a *unidirectional* antenna (and wide for omni-directional) and therefore this characteristic has not been included in the table.

Type	Gain (dBi)	Radiation	Bandwidth	Size
0.5λ Dipole	2.15	Omnidirectional	Medium	Medium
Monopole	5.15	Omnidirectional	Small	Small
Helical	< 20	Either	Large (50 - 60%)	Small-Medium
Microstrip	< 10	Either	Small-Medium	Small
Yagi-Uda	< 40	Unidirectional	Small	Large

Table 2.1: Qualitative Comparison of Antenna Characteristics [7]

2.4 Telecommunication

A brief review of various concepts used in wireless communication links is conducted below.

2.4.1 Modulation Techniques

The *modulation* technique used over a communication link refers to the method used to encode analog or digital information into an electrical voltage. ASK, FSK, PSK, and QAM are the most common techniques [17] [18]:

- *Amplitude Shift Keying* (ASK). This technique modulates the amplitude of the voltage to represent various bit levels.
- *Frequency Shift Keying* (FSK). This method changes the frequency of the signal to represent various signal levels. Commonly, *Gaussian-FSK* (GFSK) is used, which implements a smoothing filter. This decreased the bandwidth for similar throughput, making it comparable to the following techniques.
- *Phase Shift Keying* (PSK). This is often seen as a variation of FSK, where the phase of the signal is varied instead of the frequency. It requires complex synchronisation, and has lower spectral efficiency compared to QAM.
- *Quadrature Amplitude Modulation* (QAM). This method modulates both the amplitude and phase of a signal, allowing for a large number of signal levels. It has very high spectral efficiency, and is commonly used for high cost, high throughput systems.

LoRa (”Long-Range”) modulation is a relatively new technique. It makes use of frequency-varying ”chirps” to modulation the incoming signal. It has been seen to drastically increase range capacity, at the expense of greater bandwidth requirements [19]. Its practical use has also been demonstrated in an existing CubeSat system [20].

2.4.2 Link Budget

For any communication system, a ”link-level” design or *link budget* should be conducted. The goal of this design step is to determine the power requirements of the commuication system, taking into account transmitter power, antenna characteristics, receiver sensitivity, modulation technique, and any attenuation involved.

A number of the attenuation affects which may be taken into account in a satellite link budget include [21]:

- Cable loss
- Amplifier-antenna mismatch
- Free-space path losses
- Absorption losses due to clouds, rain etc.
- *Polarization* mismatch due to antennas not being aligned
- *Scintillation* effects due to changes in the air’s refractive index
- The effect of varying *elevation angles*

Further, it is recommend to include a minimum margin or *fade margin* of at least 3 dB for low frequency links [22], up to 10 dB for links that require more up-time [23], and around 20 dB for mission critical links.

2.4.3 Protocols

A few link-layer and network-layer protocols exist that facilitate nano-satellite applications. The CubeSat Space Protocol (CSP) [24] is a fully-fledged network delivery protocol for CubeSats, embedded systems, and similar. It allows for all devices in the PocketQube ecosystem (all PQ modules, the ground station, a control computer etc.) to communicate ”directly” via packet forwarding etc. It relies on various link-layer protocols, such as I2C, CCSDS (*Consultative Committee for Space Data Systems*) as its foundation. For this project, considerations will need to be made as to whether or not these protocols are applicable, or if more custom solutions should be developed.

3. System Design

3.1 Overview

This chapter encompasses the system-level design. The approach is to make design choices that allow for modularity with regards to component integration and testing. The specific details of the circuit design and interconnects will be not be discussed, however initial high-level design choices will be made. This include decisions for the overall system, the PocketQube unit, and the ground station unit.

3.2 High-Level System

There are various decisions to be made regarding the entire communication system. A complete high-level system block diagram illustrating the decisions discussed below is shown in Figure 3.1. Note that the yellow blocks are external (i.e. assumed to be available already).

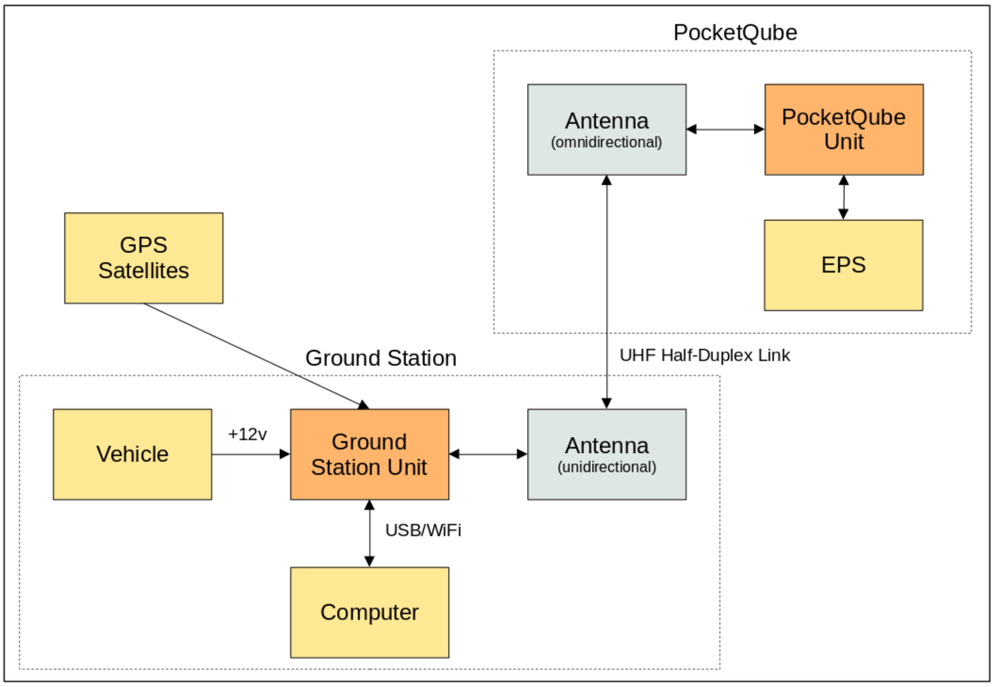

Figure 3.1: High-Level System Diagram

3.2.1 Methodology

Since a large number of sub-systemS are required on the ground-station, either IC *modules* or simple *reference designs* will be form the basic building blocks of the system. This will simplify the design process and integration. Only if no modules or designs are found to meet the system requirements, should a more custom solution be developed. The ground station will be powered via +12V from a nearby vehicle, and the PocketQube will be powered from an on-board EPS (another PQ unit). Both sub-systems should be designed such that testing without a vehicle/EPS is also possible.

3.2.2 Tracking

It is assumed that open-loop path-predicted tracking is generally adequate for high-altitude balloons, given the number of tools available to predict their flight path. In this sense, the ground station requires at least a GPS connection, as well as a means of determining true north (such as a magnetometer) for beem steering. The path data will be uploaded to the ground station via USB from a system *computer*. Further, this computer will be used to monitor the link and record the data. If time allows, direct GPS tracking will be added as a method of ”closing the loop”, and to improve pointing accuracy.

3.2.3 Custom Protocol

Half-duplex communication will be designed for, since full-duplex is assumed to be unnecessary for this type of link. This is due to the nature of the link itself (i.e. downlink telemetry), as well as a simple command-response (”telecommand”) pattern that would be used for bi-directional communication. For the given flight path, a goal of at least 9600 downlink baud rate will be designed for at the approximate 110 km range. LoRa will be explored further as the main modulation technique in the detailed design stage, however a secondary scheme such as GFSK should be considered as a backup, which is well-estabilished and is considered suitable over such a range. The 433 MHz amateur band (430 to 440 MHz) will be utilized.

3.2.4 Radiosonde Protocol

The requirement to communicate with the existing Radiosonde should be considered. According to the iMet54’s datasheet [9], it operates at a centre frequency of between 402 and 405 MHz, selected in 1 MHz increments. Ideally, for a simpler design, one antenna should be designed on the GS supporting both the custom and radiosonde communication communication protocols. The feasibility of this will be investigated further in the antenna design stage.

3.3 Ground Station

A block diagram of the system components for the ground station is shown in Figure 3.2.

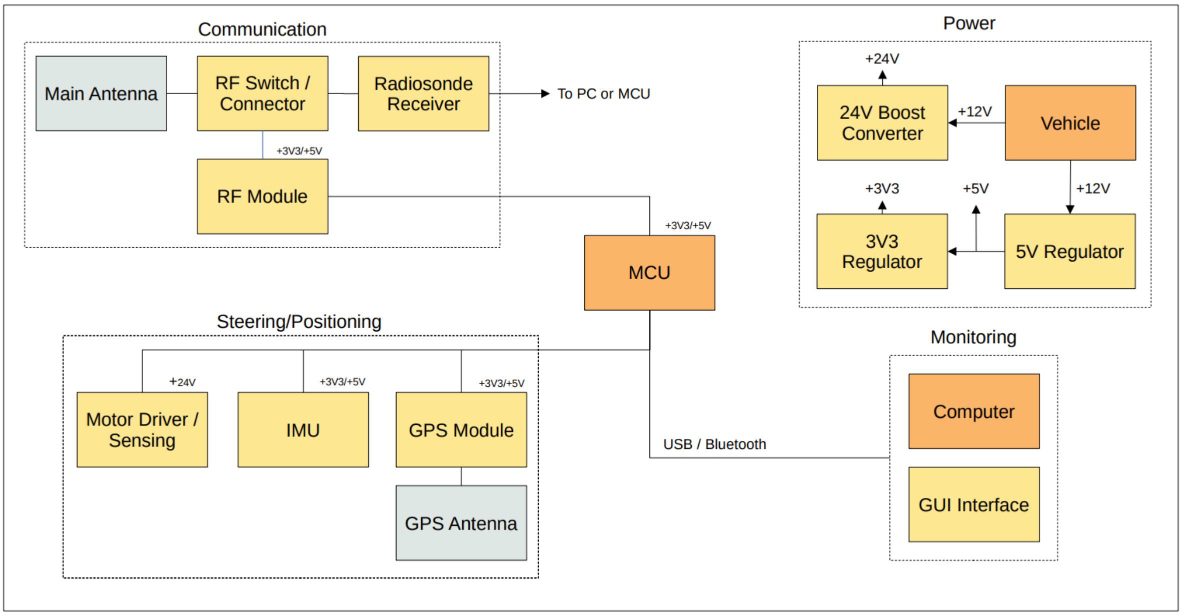

Figure 3.2: Groud Station System Diagram

3.3.1 Power

The power section consists of two linear regulators, as well as a boost converter. The existing antenna mount has two *NEMA 17 4218S-15* stepper motors, which will be used to steer the ground station in the direction of the satellite. These motors are ideally powered from +24V, and therefore a boost converter will be used to step up the voltage from the car's voltage of +12V. Further, +5V and +3V3 regulators will be included to power both the MCU and any other ICs (depending on the voltage levels). This is as the efficiency requirements of the system are low, and the current consumption of the ICs (MCU, RF module etc.) is assumed to be relatively low as well.

3.3.2 Communication

The communication section consists of the main antenna, as well as the RF control circuitry and connectors. The *RF Switch/Connector* is provided to allow the antenna to be shared between the custom and radiosonde communication links. Initially, a connector will be used for prototyping. Then, if time allows, a dedicated RF switch will be included, which will allow for the MCU to control the antenna connection. Both the RF module and the radiosonde receiver will connect through the RF switch/connector and to the antenna. The radiosonde will either connect to the PC (e.g. if an SDR dongle is used) or to the MCU (if a dedicated receiver is used).

3.3.3 Steering and Positioning

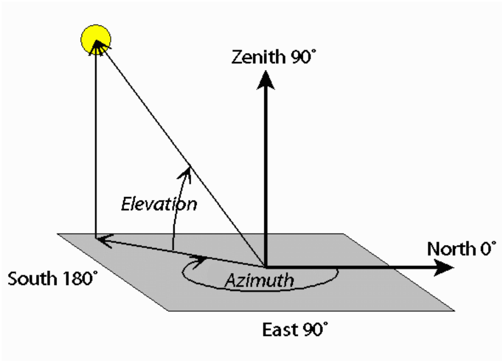

Figure 3.3: Azimuthal and Elevation Visualization [6]

Generally, the orientation of a ground station's antenna is described by both an azimuthal and an elevation angle, as in Figure 3.3. The resultant two angles should be controllable to a reasonable degree of accuracy, such that the antenna can point in a given direction.

The existing two-axis antenna mount is shown in Figure 3.4. Since the antenna platform moves relative to the base (where the PCB is mounted), this relative angle needs to be known. Two options to do this are considered:

1. *Open-loop.* The base's absolute orientation is measured/known, and the platform's relative orientation is calibrated and calculated/looked up based on the stepper motor positions.

2. *Closed-loop.* The platform's absolute orientation is measured in realtime, and this information is fed back into the motor's control system to point the platform correctly.

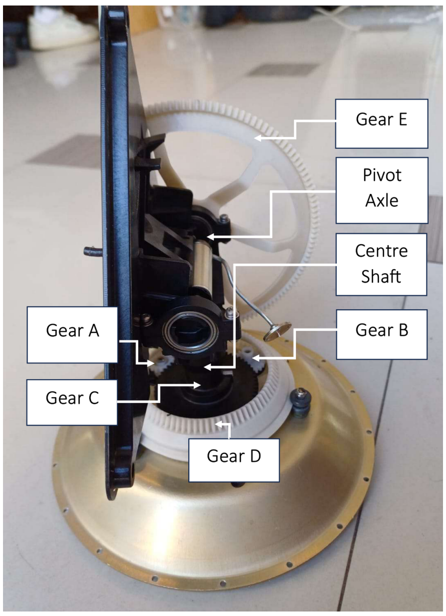

Figure 3.4: The Existing Antenna Mount

Since stepper motors are available, the *open-loop* method will be considered, however the closed loop method may be implemented if this method is found to lack accuracy, or the motor locations are found to be unpredictable, during testing. In this case, an inertial measurement unit (IMU), which typically includes an accelerometer and gyroscope, will be used.

3.3.4 Monitoring

A laptop or PC will be used to monitor the connection. A Graphical User Application (GUI) will be implemented for ease-of-use. This will include the following functionality:

- Send commands to the ground station and/or satellite.
- Read telemetry of the satelite.
- Control the ground station orientation e.g. performing motor calibration etc.
- Set communication parameters e.g. output power and modulation parameters.
- Monitor communication link performance.

3.4 PocketQube Unit

A block diagram of the system components for the PocketQube unit is shown in Figure 3.5.

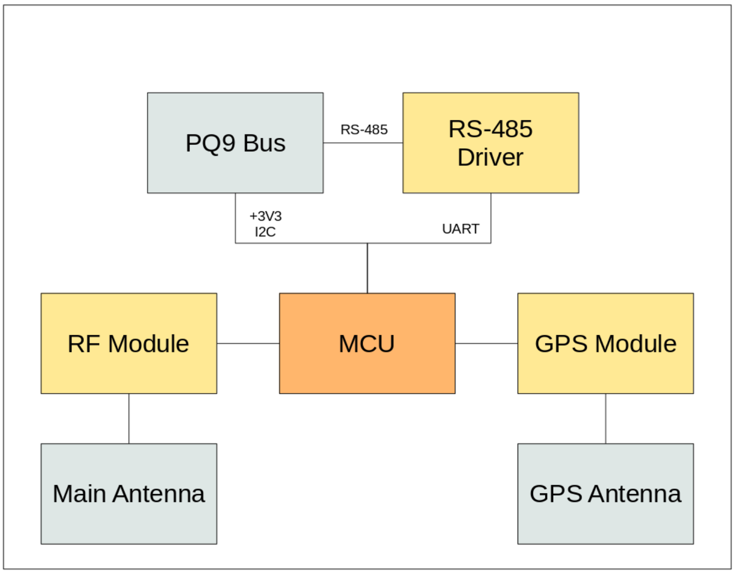

Figure 3.5: PocketQube Unit System Diagram

This unit is relatively simple in comparison to the ground station, and so the ground station should be considered a priority. The unit consists of an RF section, and a GPS section. The RF antenna should integrate well onto a typical PocketQube housing, as should the GPS antenna. The MCU should be capable of interfacing with the Stellenbosch PocketQube bus, which includes:

- A 3V3 line
- A 5V line
- An I2C bus
- An RS-485 bus

The MCU will pull directly from the +3V3 line, and will also communicate directly with the I2C bus. However, an RS-485 line transceiver should be included to cater for the RS-485 protocol, which will connect to the MCU via UART.

4. Detailed Design

4.1 Component Selection

The first step in the detailed design process is to select components for the various sub-systems. Components for both the ground station and PQ unit will be selected in one step, due to the overlapping research involved. Ideally, components should be readily available from local suppliers. Finally, through-hole components and breakout boards will mostly be used for the ground station, and surface mount components for the PQ unit.

4.1.1 Existing Components

The ground station has a number components which will be used without modification. As mentioned, two stepper motors are already mounted. These motors draw 0.50 A, and allow for up to $0.5\,\mathrm{N} \cdot \mathrm{m}$ of torque [25]. The ground station also includes a small zero-sensing circuit for the azimuthal direction, which integrates a *H22A* optical switch [26] and a low-pass filter.

4.1.2 GPS

The same GPS will be selected for both the ground station and PQ unit to simplify development. A 1 degree pointing accuracy will be designed for, which is an order of magnitude larger than any typical narrow-beam antenna. A distance of 110 km therefore results in a required accuracy of $2 \times 110000 \times \pi \times \frac{1}{360} \approx 2\,\mathrm{km}$, which is very large.

The NEO line of GPS modules from *u-blox* (e.g. the *NEO-6M*) are very commonly used, and are quoted to have a 2.5 m accuracy, however there was limited availability of these modules from local suppliers at the time of ordering. Modules with similiar specifications from *Makerbase* were therefore considered, such as the *ATGM336H* and the *ATGM332D*. Since both of these advertise 2.5 m accuracy, active antenna support, and current consumption less than 100 mA, the ATGM332D-5N31 was chosen for its lower price.

4.1.3 IMU

To determine absolute azimuthal rotation, the ground station (either the base or the platform) should either be manually positioned to face north, or a magnetometer may be used. Further, to allow for further flexibility, the ground station may be mounted on a tripod. In this case, an intertial measurement unit (IMU) may be needed to determine the mount's absolute rotation.

As seen in Section 4.1.2, low accuracy is required. A low-accuracy IMU will therefore be included, with an accelerometer and magnetometer. The *BNO055* is a 9-axis IMU which integrates an ARM Cortex-M0 for signal processing. It operates at 100 Hz, has 0.3 µT magnetic field resolution, and around 16 bit sensors. It is, however, very expensive (around R800). The *MPU-9250*, and the *MPU* line of IMU's are seen as cheaper alternatives. Since the ground station's mount will not be moving, only an accelerometer is adequate for orientation. The MPU-9250 also has a 16-bit accelerometer, and only a slightly lower magnetic field accuracy (0.6 µT), and therefore was purchased at a price of around R150.

4.1.4 RF Module

The transciever for both the custom and radiosonde protocol needs to be considered. There are a few options in this regard, listed from more to less specialized:

- Fully custom design. Here, all components are discretely designed using transistors, MCUs etc. This option is listed for completeness, but is out of the scope of this project.

- Front-End Module (FEM). For this option, the FEM provides filters, a low-noise amplifier (LNA), antenna matching, and down-conversion. Then, a controller (e.g. FPGA or MCU) needs to be designed to perform modulation/demodulation functionality (the *modem*) and interface with the FEM.

- Dedicated Transciever. A transciever provides both the FEM functionality and the software modulation, however still requires RF techniques for matching, as well as an additional RF shield.

- Dedicated module. For this option, all functionality is provided in a dedicated modulate with an antenna and MCU interface. This method has little flexibility, since all matching is done internally and the frequency band is therefore constrained.

- Software-defined radio (SDR). This is the most general-purpose option, but does not exercise the highest performance. It is often directly connected to a computer.

Custom Communication

For the custom protocol, a dedicated LoRa module will be used. Most of these modules have the added benefit of allowing GFSK modulation as an alternative. Unfortunately, few modules exist that allow for reception both in the 404 MHz and the 433 MHz bands. Table 4.1 contrasts the two most common modules in the 433 MHz LoRa band which offer this feature. Most modules available are based on *Semtech* chipsets due to the company's patent on the technology, and so there is little variation in performance. The RA-02 is therefore selected due to its availability and cost.

Name	RX Sensitivity	TX Sensitivity	Frequency
RA-02	-141 dBm	+17 dBm	410 to 525 MHz
RFM98	-148 dBm	+20 dBm	410 to 525 MHz

Table 4.1

Radiosonde Communication

Since the radiosonde communication protocol will require some investigation, and the exact encoding and GFSK parameters are unknown, SDR will be utilized to allow for flexibility. Universal Radio Hacker (URH) (https://github.com/jopohl/urh) is software available to investigate wireless protocols using an SDR. The "RTLSDR" is considered the standard, low-cost solution for this, and will be used.

4.1.5 Stepper Motor Driver

The original PCB of the previous antenna mount system contained two A3972 ICs to drive the stepper motors. Although these could be de-soldered and used, it is favourable to use a newer supported IC with better capabilities, and in case of damage. From the driver and motor datasheets, the following specifications are realized:

- Dual DMOS Full-Bridge Output Configuration
- Bipolar PWM current control
- Micro-stepping (for smoother stepping)
- 0.5A, 24V

Very few drivers fit these exact specifications. The *A4970* is considered the follow-up version of the *A3972*, however is not available in a single pack. The L6219 driver is found to match these specifications and will be selected due to availability.

4.1.6 Power

Both a 3.3V regulator and 5V regulator will be needed for the ground station power distribution. The LD1117V33C and L7805CP are chosen respectively due to their availability. A boost converter will also be needed to achieve the 24V motor drive voltage. Since each stepper motor will draw around 0.5 A per coil, the converter should support 2 A at its 12 V input. A breakout board based on the XL6009 IC will be used which meets this specification.

4.1.7 Microcontroller

As discussed later, a general-purpose MCU will be needed both on the GS and the PQ. The three most popular frameworks/MCU types for this the ESP32, Arduino, and STM32.

The *ESP32-WROOM-32* is a commonly available ESP32 variant which has 32 GPIO pins, of which several can be used as an ADC input, SPI or I2C interface. This means that there are 23x GPIO available, enough for this project. Further, the ESP32 has the added benefit of WiFi and Bluetooth connectivity, which may allow "smart" features to be added to either devices in the future. The *ATMEGA328PB* is an MCU commonly used in small Arduino boards. It, however, has fewer pins than the ESP, is an 8-bit MCU, and has only 32 KB of flash memory.. It does, however, allow a supply voltage of as low as 1.8V. Finally, the common *STM32F411* MCU is a high-performance, ARM-Cortex board with highly accurate ADCs, up to 81 GPIOs, and a fast internal FPU.

Since the processing requirements for this project are not very high, and the ESP32 is a relatively high-performance MCU which satisfies the pin requirements and has added smart capabilities, it will be selected for the GS. For the PQ unit, an ATMEGA328PB will be used, due to its exceptionally low current consumption, and many fewer pins being needed for the PQ unit.

4.1.8 RS-485 Driver

Most RS-485 drivers come in a common 8-pin form factor. Due to having very little requirements (i.e. short range communication, no speed specifications) the *SN75179BDR* is selected due to its availability.

4.2 Ground Station PCB

4.2.1 Circuit Design

Since the ground station mainly consists of various sub-systems and components, "typical application" circuits found in component datasheets were mostly employed. The final schematic is found in Appendix B.1.

Power

Current calculations should be done to ensure that the voltage regulators and the boost converters can provide enough power where necessary. A car socket can supply up to 10 A at +12 V (i.e. 120 W). The supply voltage, current consumption, and power consumption of the various system components is listed in Table 4.2. In all cases, maximum current is provided.

Therefore, maximum consumption - even at full motor current draw - is only 50 W, and will not place heavy load on the car socket battery supply. The 3.3 V regulator should be capable of supplying around 130 mA, and the 5 V regulator around $120\,\text{mA} + (130\,\text{mA} \times \frac{3.3\,\text{V}}{5\,\text{V}}) \approx 210\,\text{mA}$. The LD1117CV can supply up to 800 mA, and the L7805CP up to 1.5 A, meaning the limitations are met.

Component	Voltage	Current	Power
Motors	24 V	0.5 A (x4)	48 W
ESP32 Dev Board	5 V	120 mA	660 mW
RA-02	3.3 V	100 mA	330 mW
ATGM332D-5N31	3.3 V	25 mA	82.5 mW
MPU-9250	3.3 V	3.7 mA	12.21 mW

Table 4.2: Ground Station Component Power Consumption

The power section also includes selector jumpers to isolate it from the rest of the board. In this way, if a component is damaged during implementation, or if the power section is found to not be working, external power can be supplied appropriately.

Motor Drivers

The L6219 drivers require a reference voltage to set the maximum current. According to the datasheet [27], a peak current of $I_{max} = 10 \times \frac{V_{ref}}{R_s}$ in mA is used. Since the recommended value of $R_s = 1\,\Omega$ is being used, $I_{max} = 10 \times V_{ref}$ mA. Since the motors allow up to 500 mA per winding, a current value of $I_{max} = 475\,\text{mA}$ is chosen to prevent damaging the motors. Therefore, $V_{ref} = 4.75\,\text{V}$. This can be implemented with a voltage divider. Setting the upper resistor $R_1 = 1\,\text{k}\Omega$ results in $R_2 \approx 20\,\text{k}\Omega$, as shown in the schematic. The disadvantage of this method is that the maximum current cannot be controlled dynamically. The reference voltage can be replaced with a DAC from the MCU if more control is required.

Connectors

The RA-02 RF module states that not all data pins are necessary. A connector is provided for unused GPIO pins, the SPI, and the unused RF module pins, to allow for flexibility once the PCB is manufactured.

4.2.2 PCB Design

Stackup

A 2-layer stackup was decided on, so that the board could be manufactured in-house early on in the project (as the in-house PCB machine has a 2-layer limitation).

Final Design

The final PCB was designed in KiCAD. It was designed to have be compatible with the mount i.e. with a 198 mm outer diameter, outer mounting holes, and cut-outs for the stepper motors. The front layer of this design is shown in Figure 4.1. Female headers were used for most of the modules, since development boards were being used. Two PCB pours were exposed below the voltage regulators for added heat dissipation.

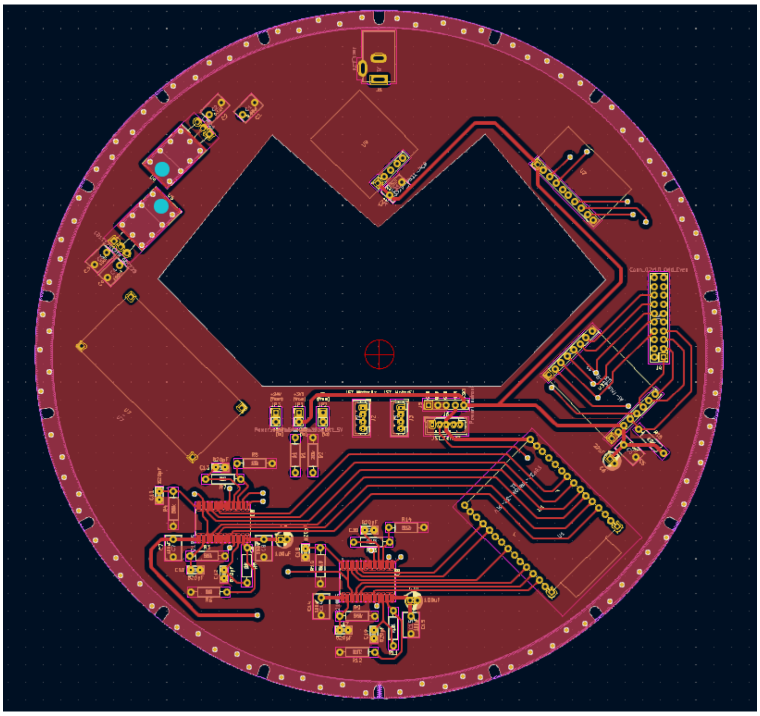

Figure 4.1: Ground Station PCB Design

4.3 Ground Station Antenna

4.3.1 Mechanical Considerations

The existing antennna mount is shown in Figure 3.4. Azimuthal and elevation stepper motors are connected directly through Gear A and B respectively. Gear A rotates the centre shaft to provide azimuthal steering, whereas Gear B rotates through Gear D and E to allow a change in elevation. The specifications in Table 4.3 were realized.

Component	Specification
Motor	200 full steps (per 360 degrees)
Gear A	15 teeth
Gear B	20 teeth
Gear C	60 teeth
Gear D	92 inner teeth, 80 outer teeth
Gear E	140 teeth (equivalent)

Table 4.3: Mount Component Specifications

The black plastic platform is triangular and has three mounting holes. The new ground station's antenna should therefore be mounted onto this platform. It is important to consider the forces/torques involved, as well as the stepper motor holding torques, in order to determine the maximum weight and acceptable form factor of the new antenna.

The azimuthal motor need not be considered, as all torques from the mount to its base are perpendicular to the central shaft, meaning it would only need to overcome static frictional forces to rotate the antenna, which are assumed to be negligible. The holding torque of the elevation motor, however, will constrain the antenna design. The holding torque of each motor is 0.25 Nm. The gearing ratio resulting from Gears B, D and E, results in an around 8x torque increase. This provides a holding torque of around 2 Nm at the pivot axle.

The centre of gravity of the antenna, as well as its weight, will affect the motor's ability to hold it in place. The horizontal distance between the pivot axle and the mount in the upright position is measured to be 40mm. Therefore, in the worst-case (when the mount is upright as in Figure 3.4) a planar antenna could weigh up to $\frac{2}{(9.8 \times 0.04)} = 5.1\,\mathrm{kg}$. In general, the "mass-distance" product of the antenna (mass times distance of centre of gravity from mount) should not be more than $0.2\,\mathrm{kg} \cdot \mathrm{m}$. This should be strongly considered if a longer antenna is desired.

The physical dimensions of the antenna's ground plane is also constrained. A circular ground plane may make contact with the mount's base at low elevation angles (assuming the ground station itself is raised above the ground). When the mount is resting, this constraint is imposed when the ground plane first makes contact with the mount's base. For a circular ground plane, this is around 360 mm diameter at an elevation angle of around 35 degrees.

4.3.2 Theoretical Design

As discussed, the antenna should be capable of receiving from both the 405 MHz radiosonde protocol, as well as the custom LoRa-based protocol in the amateur radio band of 430 to 440 MHz. A helical antenna is suggested, for the following reasons:

- Ability to increase gain arbitrarily by increasing the number of windings
- High fractional bandwidth of 56%, which may allow for a smaller antenna than other antenna types
- Ease of manufacture

The centre frequency f_c of the antenna should first be selected. With a fractional bandwidth of 56%, the inequality $f_c \times (1 - \frac{0.56}{2}) < 405\,\mathrm{MHz}$ must hold. This gives an upper bound on the centre frequency of 562.5 MHz. A minimum ground plane diameter of no smaller than 0.5λ is recommended in [13], and 0.75λ in [28]. It is, however, probable that a ground plane as small as 0.5λ will adversely affect the radiation pattern near the end of the specified bandwidth.

Assuming the larger ground plane recommendation, the resulting ground plane diameter is $0.75 \times \frac{3e8}{562.5e6} = 400\,\mathrm{mm}$, which is larger than the mechanical size constraint. Neverthless, $f_c = 550\,\mathrm{MHz}$ is chosen as the initial centre frequency for simulations. the ground plane will then be decreased in size appropriately (towards $G_\lambda = 0.5$ i.e. $270\,\mathrm{mm}$) and the results observed.

The design parameters for a helical antenna are f_c (centre frequency), n (number of turns), S (the spacing between turns), C (the circumference) and G (the ground plane diameter).

Design formulae are provided in [13], and have been modified below to use relative values instead of absolute ones (i.e. S_λ and C_λ instead of S and C). Directivity, in dBi, is given by:

$$D_0 = 10\log(15 \cdot nS_\lambda \cdot C_\lambda)$$

C_λ is typically kept at 1.0, meaning the cirumference is equal to the operating wavelength. As mentioned, a gain of around 5 dBi is required. However, a 3 dB bandwidth drop is estimated nearer to 400 MHz since it as the edge of the operating band. Further, the effect of a smaller ground plane will likely decrease performance by an estimated minimum of at least 1 dB. Therefore, a centre-frequency gain of 8 dBi will be designed for. For this gain, the nS_λ product should equal around 0.45. Although the optimal value for S_λ is 0.23 [13], smaller values have been quoted to work [15] and are mechanically easier to construct. Therefore, $S_\lambda = 0.15$ is chosen, and finally, $n = 3$.

4.3.3 Simulation Design

Simulation of a helical antenna is well documented in literature, and therefore the parameters can be varied iteratively and integrated into the antenna design process. For this project, FEKO software is used. An initial model with the above parameters, a large ground plane ($G_\lambda \approx 1.0$), and a wire diameter of 2.5 mm (chosen due to availability) is simulated. The resulting radiation pattern at the centre frequency of $f = 550$ MHz is shown in Figure 4.2, with a maximum gain of around 9.5 dBi.

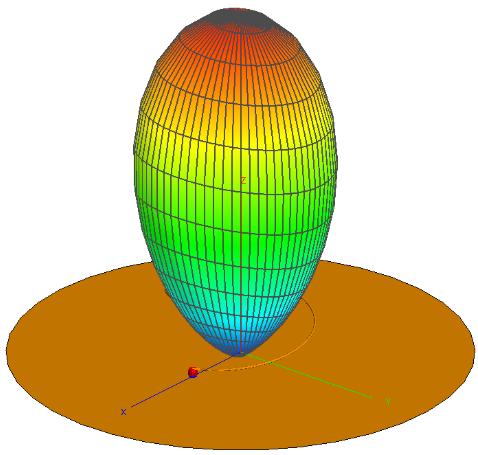

Figure 4.2: Initial Helical Antenna Radiation Pattern ($f = 550$ MHz)

Most of the initial design is conducted around the lower frequency of $f = 405$ MHz. The radiation patterns for $G_\lambda = 0.5$ and $G_\lambda = 0.7$ ($G = 273$ mm and $G = 382$ mm) are shown in Figures 4.3 and 4.4 respectively. It is clear that the recommended value of $G_\lambda = 0.5$ from [13] will not work near this lower frequency, as shown by the morphed radiation pattern. The pattern is found to be acceptable at around $G_\lambda = 0.7$. However, after analysing the input impedance for this ground plane size (shown in Figure 4.5) it is clear that broadband matching would be difficult, due to the drastic change in impedance near the lower end of the spectrum.

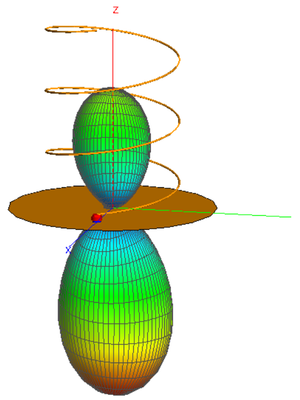

Figure 4.3: Helical Antenna Pattern at $f = 405\,\text{MHz}$ ($f_c = 550\,\text{MHz}$, $G_\lambda = 0.5$)

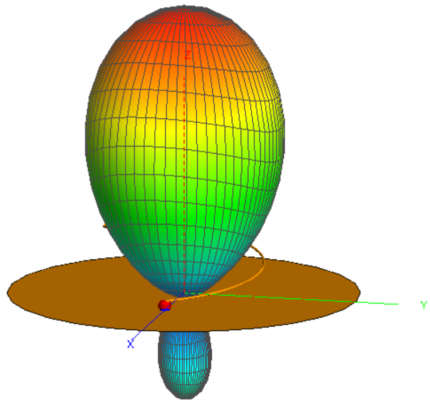

Figure 4.4: Helical Antenna Pattern at $f = 405\,\text{MHz}$ ($f_c = 550\,\text{MHz}$, $G_\lambda = 0.7$)

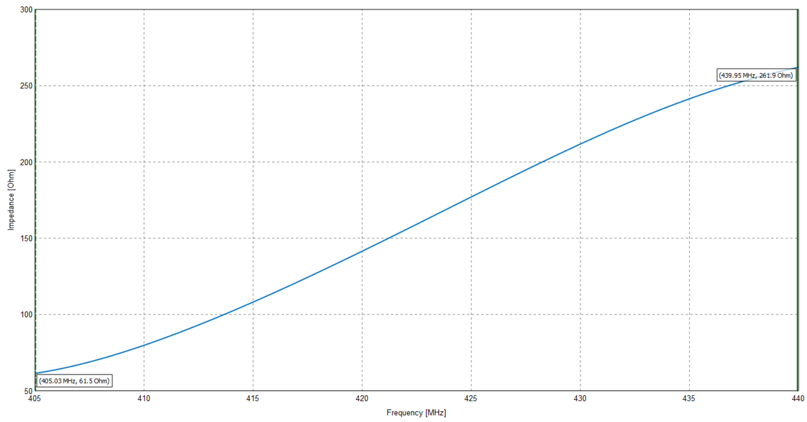

Figure 4.5: Helical Antenna Input Impedance ($f_c = 550\,\text{MHz}$, $G_\lambda = 0.7$)

The common amateur band frequency of 433 MHz is chosen for the LoRa communication link. In order to ease matching, a lower centre frequency should ideally be used, to move the input impedance at 405 MHz and at 433 MHz closer together. This will, however, require either a larger ground plane, or a cupped ground plane (discussed further on).

Unfortunately, FEKO does not allow for an optimization goal that depends on two frequencies. Therefore, an iterative approach was used to find the centre frequency which minimizes the difference between the two impedances. The resulting centre frequency was found to be around $f_c = 510\,\text{MHz}$ at $G_\lambda = 0.6$ ($\approx 350\,\text{mm}$), with a resultant input impedance close to $250\,\Omega$, as shown in Figure 4.6.

Since the mount can support a larger weight than the 3 turn coil, it was decided to experiment with larger a turn count (i.e. $n = 4$), both for increased directivity/performance, and to potentially cater for manufacturing imperfections, such as a thin aluminium foil ground plane, and any diversions from the ideal helical shape. It was found that, for small ground plane diameters, the radiation pattern for $f = 405\,\text{MHz}$ was negatively affected as the number of turns increased. This is intuitive when referring to image theory, as the non-idealities due

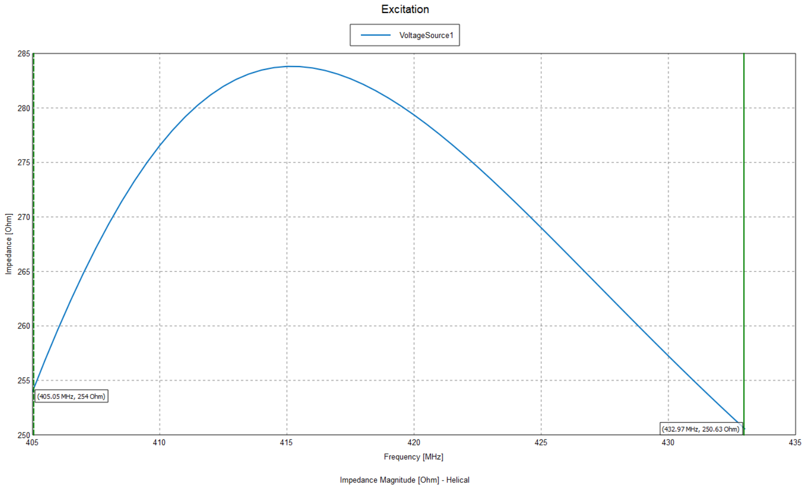

Figure 4.6: Helical Antenna Input Impedance ($f_c = 510\,\text{MHz}$, $G_\lambda = 0.6$)

to the finitely-sized ground plane become more apparent as distance to the plane increases. It should be noted that the pattern at $f = 433\,\text{MHz}$ was not as badly affected.

The ground plane was therefore cupped, and the results observed. At $G_\lambda = 0.6$, a cup height equal to 1 helical turn was found to greatly improve the radiation pattern. This is shown in Figures 4.7 and 4.8. The gain, however, was not as drastically affected.

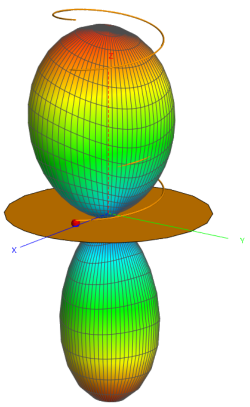

Figure 4.7: Helical Antenna Pattern without Cup ($G_\lambda = 0.6$, $f = 405\,\text{MHz}$)

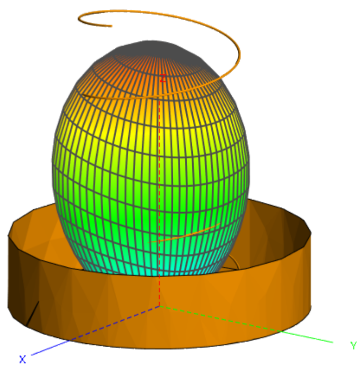

Figure 4.8: Helical Antenna Pattern with Cup ($G_\lambda = 0.6$, $f = 405\,\text{MHz}$)

It was therefore decided that the antenna would initially be built with a large ground plane and higher number of turns. Then, after measurement results and protocol implementation, the ground plane would be decreased appropriately to fit onto the mount. If time allows and it is found to be necessary, a cup will then be added to the ground plane, to improve the pattern and antenna performance, and cater for the radiosonde protocol. The final model parameters are then:

- $C_\lambda = 1.0 \therefore D = 187.1\,\text{mm}$
- $S_\lambda = 0.15 \therefore S = 88.2\,\text{mm}$
- $n = 4$

- $G_\lambda = 0.6 \therefore G = 350\,\text{mm}$

4.3.4 Matching

Impedance matching should be done if the helical antenna is to be fed by a $50\,\Omega$ coaxial cable. It was decided to match the antenna to the custom protocol's frequency of $f = 433\,\text{MHz}$ using the strip method mention in Section 2.3.2 for an uncupped ground plane. The FEKO model for this method is shown in Figure 4.9.

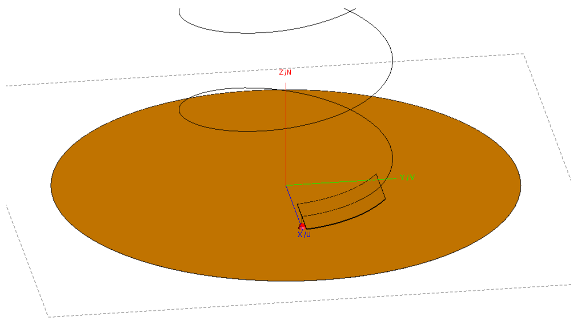

Figure 4.9: Helix Antenna Model with Matching Strip

The strip is recommended to be relatively flat, and extend for approximately the first quarter turn. Its pitch angle was therefore chosen to be half that of the full helix, and it was chosen to extend for 0.15 turns. The unknown parameters for the strip are then its height above the ground plane (also the height of the coaxial pin), and its strip width. The FEKO optimizer was used to optimize these two parameters for a minimum return loss. The resulting return loss as a function of frequency is shown in Figure 4.10. The resultant mismatch loss is close to 0 dB at the target frequency, and 0.451 dB at 405 MHz.

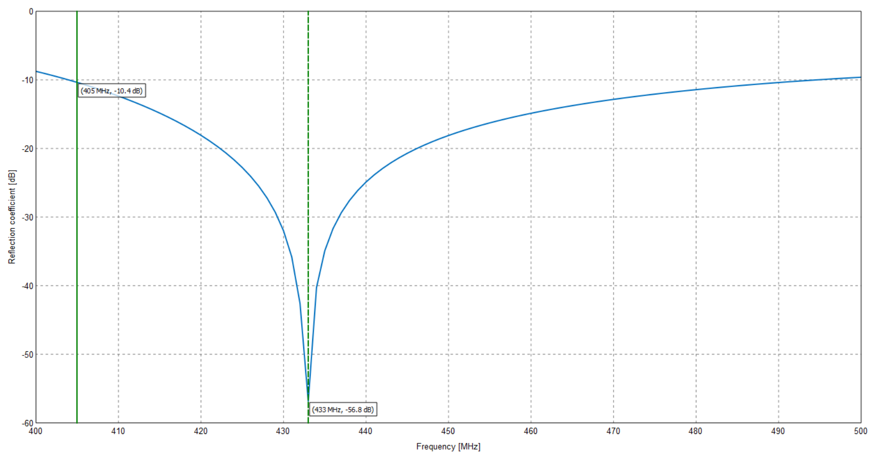

Figure 4.10: Helical Antenna Return Loss vs Frequency

The final antenna parameters are:

Parameter	Value
Diameter (D)	187.1 mm
Turn Spacing (S)	88.2 mm
No. of Turns (n)	4
Ground plane diameter (G)	> 350 mm
Strip height (sh)	19.4 mm
Strip width (sw)	77.7 mm
Strip length (sl)	132 mm
Cup height, if used (ch)	88.2 mm

Table 4.4: Helical Antenna Final Parameters

4.4 PocketQube Unit

4.4.1 Circuit Design

To design the PocketQube PCB, since no development boards were used, the Arduino Nano schematic in [29] was consulted as a reference design. It was decided to simply expose the relevant pins needed to flash the MCU, instead of integrating a USB connection directly, however this could be added for future iterations. The final circuit schematic can be found in Appendix B.2.

Power

The maximum power consumptions of the on-board components is found in Table 4.5. A total maximum power consumption of around 600 mW is calculated. This equates to around 200 mA draw for a 3.7 V LiPo battery. To achieve the 2 hour specification, a capacity of 400 mAh is therefore required. A larger 2000 mAh battery was acquired for development.

Component	Current	Power (@ 3V3)
ATmega328	12 mA	39.6 mW
RA-02	100 mA	330 mW
ATGM332D-5N31	25 mA	82.5 mW
SN75179B	57 mA	188 mW

Table 4.5: PocketQube Unit Component Power Consumption

RF

Since the RA-02 RF module has a u.FL connector onboard, no considerations need to be taken with respect to impedance matching at the interface between the module and the antenna feed. However, the ATGM332D GPS module directly exposes its RF input via one of its SMD pins, meaning impedance matching may need to be done. The higher L1 GPS band operates around 1575.42 MHz, which is a wavelength of $\frac{3e8}{1575.42e6} = 190\,\text{mm}$. The ”critical length” (the length at which reflections can be ignored) is therefore around 19 mm. Since this is relatively large, if the trace length between the module and antenna interface is kept short than this, impedance matching will not be necessary.

4.4.2 PCB Design

Stackup

It was decided to use a 2-layer board, due to the low component count. Although the impedance matching is not necessary for the GPS module, it is still desirable to control the trace impedance as much as possible. However, a 50-ohm trace on a 2-layer board is around 2.8 mm (determined using a microstrip impedance calculator), which is much larger than the pad sizes of the GPS module. Therefore, the trace was simply made as large and as short as possible.

Final Design

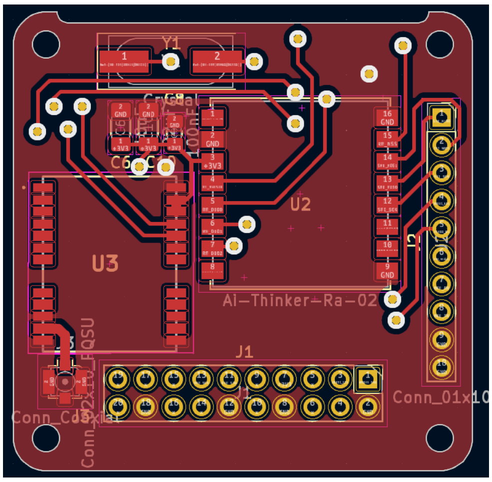

Figure 4.11: PocketQube Unit PCB Design (Front)

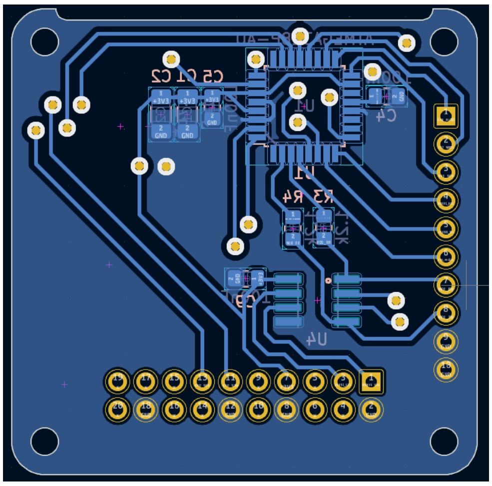

Figure 4.12: PocketQube Unit PCB Design (Back)

The final PCB was designed to conform to the PocketQube standard, as shown in Figures 4.11 and 4.12.

4.5 PocketQube Unit Antenna

4.5.1 Simulation Design and Matching

It was decided to use a simple half-wavelength dipole for the PQ unit, due to its omnidirectional radiation pattern and its extremely easy design and construction. The wavelength of interest is for the custom protocol i.e. $f = 433\,\text{MHz}$ or 693 mm. A simple 1.5 mm metal wire will be used due to its availability, with a small gap between the two sides of the dipole, and fed by a coaxial cable.

The design parameters for the dipole are L_λ (the total dipole length relative to lambda), F_{gap} (the gap distance of the feed), and F_{length}, the length of the feed. A fixed gap distance of $F_{\text{gap}} = 5\,\text{mm}$ is decided on, as it is assumed to not be critical if sufficiently small.

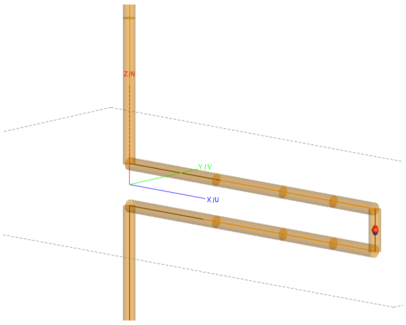

Figure 4.13: Dipole Model

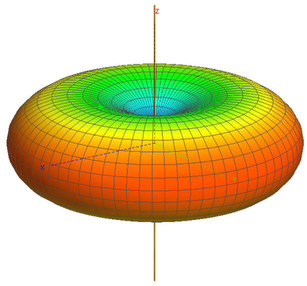

Figure 4.14: 0.45λ Dipole Radiation Pattern

The FEKO model in Figure 4.13 was used. The optimizer was used to calculate the optimal dipole length and feed length that would minimize the return loss for $f = 433\,\text{MHz}$ at a feed impedance of $50\,\Omega$. The resultant parameters are found to be $L_\lambda = 0.45$ ($L = 312\,\text{mm}$) and $F_{\text{length}} = 39.0\,\text{mm}$. The resultant radiation pattern of the dipole is shown in Figure 4.14, as well as the optimised return loss as a function of frequency in Figure 4.15.

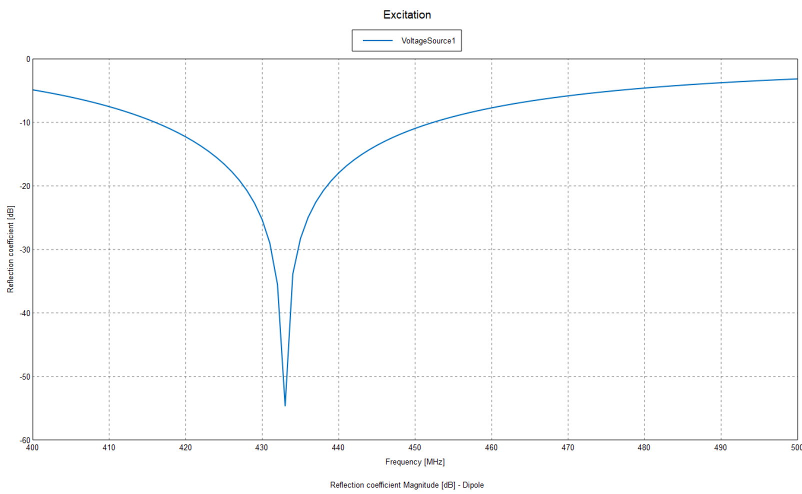

Figure 4.15: 0.45λ Dipole Return Loss vs Frequency

4.6 Link Budget

The link budget should now be conducted, and initial considerations for the ground station's base location should be made, as this location will affect the range of elevation angles to accomodate, the distance to the horizon, and the free-space path loss.

Signal Hill in Cape Town is a viable location for the ground station and is easily accessible. At its distance of 114 km, however, one would need to be at a height of 950 m due to the distance to the horizon. Therefore, the balloon would only be visible at an altitude of 600 m (from Signal Hill's 350 m height). A maximum elevation angle of 16.72$\circ$ at 30 km altitude above Worcester should be considered.

The *receiver sensitivity* is a value which denotes the minimum power level required at the receiver for successful communication. Depending on set parameters, the SX1278 quotes varying receiver sensitivity values. Notable configurations are listed in Table 4.6.

Description	**Modulation**	**Parameters**	**Bit Rate**	**Sensitivity**
Maximum Bit Rate	GFSK	62.5 kHz	250 000 bps	-92 dBm
High Bit Rate	GFSK	40 kHz	38400 bps	-109 dBm
Target Bit Rate ($\approx 9600bps$)	GFSK	5 kHz	4800 bps	-115 dBm
-	LoRa	500 kHz, SF 8	10417 bps	-119 dBm
Maximum Sensitivity	LoRa	62.5 kHz, SF 12	24 bps	-147 dBm

Table 4.6: Notable SX1278 Configurations

An online path loos calculator was used to calculate attenuation due to distance, and the Python tool *link budget* was used to calculate atmospheric losses. All values were based on both the RA-02 and the SX1278 chip specifications, as well as half-wavelength dipoles as antennas, an impedance mismatch loss of 0.5 dB (around -10 dB return loss), and an maximum transmitter power (18 dBm). The resultant link margin should then be analysed accordingly, and an appropriate directive antenna should be designed for the ground station, to ensure adequate fade margin and performance. The LoRa "target bit rate" sensitivity value of -119 dBm is used in this budget.

Transmitter Power	18 dBm
Mismatch Loss	(0.5 dB)
Transmission Line Loss	(1 dB)
Antenna Gain	2.15 dB
EIRP	**18.65 dBm**

Table 4.7: Link Budget - Satellite

Free space path loss (114 km)	126.3 dB
Atmospheric loss	0.22 dB
Scintillation loss	0.37 dB
Polarization Mismatch	3 dB
Total Loss	**129.89 dB**

Table 4.8: Link Budget - Channel

Antenna Gain	2.15 dBi
Mismatch Loss	(0.5 dB)
Transmission Line Loss	(1 dB)
Receiver Sensitivity	119 dBm
GS Sensitivity	**119.65 dBm**

Table 4.9: Link Budget - Ground Station

The final link budget therefore results in 18.65 dBm - 129.89 dB + 119.65 dBm = 8.41 dB of link margin. Although this is theoretically adequate (above the 3 dB recommendation), there are a few considerations to be made:

- If a higher bit rate is required, e.g. 38.4 kbps, then the margin drops to -2.59 dB.
- If a longer range is required (e.g. for future projects), free space path loss will drastically increase. For example, for a 250 km range, the loss becomes 133 dB, meaning the margin drops to only 1.11 dB.

To achieve the 10 dB recommended margin, an antenna with at least 2.59 dBi additional gain (i.e. 4.74 dBi total) should be designed for the ground station. Then, if necessary, the 20 dB recommendation can be reached by lowering the LoRa spreading factor (SF) to support any ”mission critical” requirements. Practically, this could be set as the system ”startup” state, until a link is made, where the SF can then be changed.

4.7 Software

4.7.1 Components

A shared library was designed in C++ to be re-used in both the PQ and GS code. Composition was used to to follow the component-based design. Tables 4.10 to 4.15 describe the various classes planned, as well as their expected functionality, with *setup/update* functions excluded.

The *Link* class deserves additional explanation. Although mature protocols exist (such as CSP as mentioned) it was decided to develop only a very simple protocol between the PQ and GS. The link class is designed to encapsulate flow control of the radio communication link, and should be configurable to either be in *Controller* or *Responder* mode (for the GS and PQ respectively). It should allow for either *Telemetry* or *Telecommand* operating modes, and allow callers to simply use callbacks to populate/respond to data when necessary.

Table 4.10: GPS Class

Function	Description
getLocation()	Return latitude, longitude and altitude
getTime()	Return seconds since epoch

Table 4.11: Radio Class

Function	Description
startTransmit(message)	Transmit data (non-blocking i.e. with callback)
startReceive()	Start listening to receive data (non-blocking i.e. with callback)
getRssi()	Get signal strength
getSnr()	Get signal-to-noise ratio

Table 4.12: Link Class

Function	Description
setTelemetryCallback(fn)	Set the ”telemetry sent/received” function
setTelecommandCallback(fn)	Set the ”telecommand received” function (*Responder* only)

Table 4.13: StepperMotor Class

Function	Description
stepForward(numSteps)	Blocking and non-blocking options
saveZeroPosition()	Used for calibration
getPosition()	Used for open-loop feedback
setSpeed()	Sets the delay between steps
setCurrentMultiplier()	Set the amount of current

Table 4.14: Mount Class

Function	Description
calibrate()	Calbrate the mount
setAzimuthalElevation(az, el)	Set the azimuthal and elevation angles
setBoresight(boresightVec)	Set the boresight pointing vector

Table 4.15: GroundStation Class

Function	Description
calibrate()	Calibrate the entire GS
addEstimatedLocation(loc)	Add an estimated input GPS location for open-loop tracking
addKnownLocation(loc)	Add a known GPS location for closed-loop tracking

4.7.2 Containers

Two larger classes were designed to encapsulate/contain the above components:

1. **PqTnc** class, which acts as an interface between the GS, and a host computer. Here, the GS is referred to as a *Terminal Node Controller* (TNC) when referring to the serial interface it exposes to a host computer. This class should contain the ground station object, handle serial commuication and errors, and store any data to provide the ground station object (e.g. GPS flight path information).

2. **PqUnit** class, which encapsulates all functionality for the PQ module, such as populating telemetry buffers, and responding to telecommands.

A protocol titled the *SUNCQ* protocol was drawn up to facilitate commands between the TNC and a computer. This can be found in Appendix C.2. Some commands were included for future contingency (e.g. the inclusion of a TNC ”mode” with support for the common KISS (Keep It Simple Stupid) protocol).

5. Implementation

5.1 Ground Station PCB

The ground station PCB was manufactured in-house. A figure of the PCB with components assembled, as well as a helical antenna attached for initial development, and a simple monopole GPS antenna, is shown in Figure 5.1. Due to a few incorrect layouts on the PCB, some additional wired connections were made. A list of errata for both PCBs can be found in Appendix B.3.

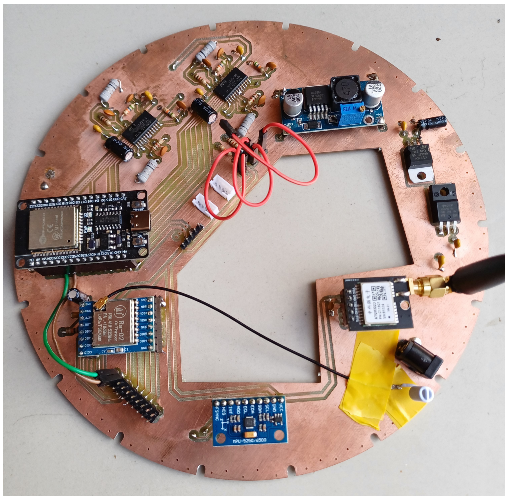

Figure 5.1: Ground Station PCB Implementation

5.2 Ground Station Antenna

The initial helical antenna build is shown in Appendix D.1. 2.5 mm stranded copper wire was used due to its flexibility and availability. A cardboad ground plane wrapped in aluminium foil was used due to its lightweight nature. Further, a strip of harder aluminium tin was taped to the wire for the matching strip. Initially, the strip was purposefully over-sized, and more turns than necessary were used. A female panel-mounted SMA connector was mounted using bolts, and the antenna wire was soldered to the protruding pin.

The coiled wire is mechanically supported by a central PVC pipe and wooden dowels. Markings on the pipe were used to dimension the antenna. The materials were sized to provide stability, but not exceed the maximum torque limitations of the motors. The final antenna weight was measured at xxx. After initial testing, the matching strip was cut to size, a circular trapezoidal ground station cut-out was made for a lower elevation angle, and the number of turns were decreased. The system was eventually mounted onto a tripod, and a final photo of the full ground station out in the field is shown in Figure 5.2.

Figure 5.2: Ground Station Mounted on Tripod

5.3 PocketQube Unit PCB

It was decided to order the PQ unit PCB, due to the higher complexity of the board. In order to begin initial development and testing, a breadboard prototype was initially created using an Arduino Nano, as shown in Appendix D.2. Since the Nano has the same MCU as the designed PCB, the developed software could then simply be flashed onto the PQ unit using an off-board programmer.

The final module is shown in Figures 5.3 and 5.4. On the PCB itself, it was noted that the two required loading capacitors were mistakingly left out for the MCU's crystal oscillator (included in the appendix errata). The MCU's internal 8 MHz clock was therefore used. This clock, however, is generally badly calibrated, and resulted in software serial communication with the GPS module initially not working. The OSCCAL register was therefore optimized to re-calibrate the clock.

The board was first bootloaded with an Arduino Nano, and then the programmer circuit below was developed to flash the board via UART. The programmer consists of a CH340 USB-to-serial module, a reset RC filter, as well as a 3.3V to 5V level converter (since the PocketQube PCB is designed to run at 3.3V).

The board and dipole antenna was mounted onto a LiPo battery. The power section

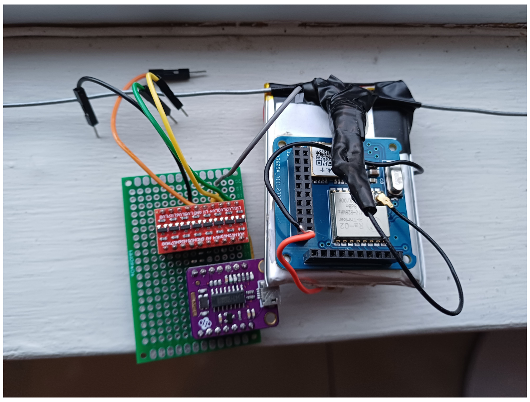

Figure 5.3: PQ Unit (front) [right] and programmer [left]

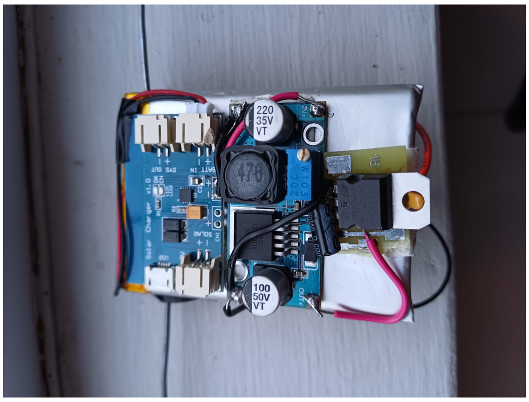

Figure 5.4: PQ Unit (back)

consists of a LiPo charger, a boost converter module, and a 3.3V linear voltage regulator circuit. This section was implemented in order to supply the PocketQube with power through the bus to allowing for testing without being connected to USB power.

5.4 PocketQube Unit Antenna

The PQ unit antenna was simply implemented using readily available 1.5 mm steel wire. The wire was bent manually and the end of u.FL pigtail cable was stripped and soldered to the wire. Lastly, insulation tape was added near the connection for stability and protection. The final design can be found in Appendix D.2.

5.5 Software

The following section documents the algorithms implemented in software to satisfying the required functionality layed out in the design stage. All code can be found at `https://github.com/gvcallen/pqcom/tree/main/code`.

5.5.1 Mount

The two-axis mount requires some relatively involved control. The end goal is to be able to set a specific azimuth and elevation angle.

Adjusting the elevation angle while keeping the azimuthal angle fixed is simple. The azimuthal motor (controlled Gear C in 3.4) can be held fixed, and the elevation axis (Gear D) stepped accordingly. For azimuthal variation, if the elevation axis is held fixed, rotating the azimuthal axis causes the mount to also change in elevation, which needs to be compensated for. The *"azel"* ratio is then defined as the number of turns the elevation motor requires to tilt the elevation by the same amount as that caused by a given azimuthal rotation. The formula for this ratio is found to be:

$$\text{azelRatio} = \frac{D_{\text{outer}}/B}{C/A} = \frac{92/20}{60/15} = 1.15 \tag{5.1}$$

The azimuthal and elevation angles can then be calculated as in Formulas 5.2 and 5.3, where *elRev* is the number of elevation motor steps per elevation revolution (equal to $200 \times \frac{92}{20} \times \frac{140}{80} = 1610$), and *azRev* the equivalent for azimuth (equal to $200 \times \frac{60}{15}$).

$$\text{azAngle} = \text{azPos} \times \frac{360°}{\text{azRev}} \tag{5.2}$$

$$\text{elAngle} = (\text{azPos} \times \text{azelRatio} + \text{elPos}) \times \frac{360°}{\text{elRev}} \tag{5.3}$$

The number of simultaneous *"delta"* steps to make for each axis to move to (newAzAng, newElAng) in *setAzimuthElevation()* is then given by Formulas 5.4 and 5.5. To do these steps simultaneously, the motor speeds can be set according to the ratio of the number of steps, ensuring there is a single, smooth movement from one position to another. Lastly, a conversion from cartesian to azimuthal-elevation is done to allow setting a boresight vector.

$$\text{deltaAzSteps} = \text{angToPosAz(newAzAng)} - \text{azPos} \tag{5.4}$$

$$\text{deltaElSteps} = \text{-deltaAzSteps} \times \text{azelRatio} + \text{angToPosDeltaEl(newElAng - elAng)} \tag{5.5}$$

5.5.2 Ground Station

Pointing

In order to point the ground station at a specified GPS location, an internal *pointAt* function was developed. A small C++ header-only library titled *wgs84* was used to perform a Mercator projection to cartesian co-ordinates, with Cape Town set as the origin. This then allowed a pointing vector to be determined, which could be passed to the mount and set as the boresight.

Unfortunately, the purchased IMU (the MPU-9250) was found to be counterfeit and did not include a magnetometer. Therefore, a constraint was made that the ground station should be manually positioned to face magnetic north using a compass, and then the zero sensor location used.

Flight Path Tracking

For open-loop flight path tracking, it was decided to store GPS path data in the TNC object on the ESP32 itself, as opposed to streaming it from the host computer. This was chosen for two reasons:

1. The host can be disconnected, and the payload will still be tracked.

2. Easier implementation on the host side (i.e. the binary GPS data can be uploaded and then ”forgetten” about)

The PqTnc class simply checks in its update loop if a location in the path has been reached based on time, and adds the following location as an estimated location to the GroundStation object. The GroundStation itself only stores two locations - the previous location in the path, and the location it is moving towards. Periodic updates (e.g. once every second) are done and the mount is pointed at a location which linearly interpolates the two stored location instants, based on the current time GPS epoch time, and the time of the two instants.

Direct GPS Tracking

To allow direct GPS tracking and flight path tracking to be used simultaneously, it was decided to follow the flight path data until a location from the satellite is received. When a ”known” location is received, it is used for a specified timeout ”trust” period, until a new location is received and it is overwritten. If the trust period expires, the method falls back to the flight path data. A pseudo low-pass filter is added to the ground station to prevent pointing ”jitter” that may occur when receiving slightly different coordinates. This filter simply does not re-point the mount if the angle is less than a specified amount (i.e. 5°).

5.5.3 Radio and IMU

For the radio and GPS classes, existing Arduino libraries were utilized and wrapped into ”cover classes”. This was done to maintain a consistent interface, and to provide the ability to replace the underlying implementation, if necessary.

Initially, the library *Radiolib* was used for communication with the SX1278 module. However, it was found that its implementation was too large for the Atmega328. It was therefore replaced with its older implementation, *LoRaLib*, which was considerably smaller in size. For the GPS, *TinyGPSPlus* was used.

5.5.4 Motor Drive

The motor’s were set to operate in half-stepping mode with a maximum current. The step sequence as in the motor driver datasheet was implemented using an array with code stepping through at regular intervals, as given in the L6219’s datasheet [27].

5.5.5 GUI

A simple GUI application was development using the Qt framework to ease testing and flight path uploading. The ability to import a CSV in the format provided by habhub was provided. An image of this application can be found in Appendix D.3.

6. Testing

6.1 Ground Station PCB

After implementation, trivial initial tests were done to ensure the ground station was functional. This included ensuring all modules (radio, GPS and IMU) could be interfaced with successfully, as well as the more detailed power tests documented below.

6.1.1 Power

During no load from the motors, but load from the integrated circuits, the voltage readings in Table 6.1 were obtained. The GPS and ESP lights were noted to be on. From these tests, is clear that the full power system is working as expected.

Component	**Expected**	**Measured**
LD1117	3.3 V	3.307 V
LM7805	5 V	5.069 V
XL6009	24 V	24.07 V

Table 6.1: Ground Station Voltage Measurements

The current consumption through a 12.3 V supply was measured at 179 mA with all systems on except the motor drive. This equates to around 2.2 W of power. Since a total of around 1 W of power is expected during no transmission as calculated previously, this implies that the voltage regulators are disippating the remaining 1.2 W. This is well within the limitations of both regulators e.g. the LD1117 can disippate a theoretical maximum of 12 W. The system was left idle for an hour with no noticeable change in current or heat.

6.1.2 Motor Drive

The motor drive system was tested with the half-step sequence implemented as previously mentioned. Current measurements were made for different operating conditions and are listed in Table 6.2. Tests 1-4 were conducted uing a *calibrate - return to stow* cycle repeated 10 times at 2/3 maximum current, and were intended to determine the speed limitations of the system, since it is easy to identify if the system misses steps by moving it back and forth continuously. Tests 5-6 were conducted with the mount stationary at around 75 degrees elevation at 2/3 and 3/3 current respectively, and were intended to stress test the current handling capabilities of the system. Note that 179 mA have been subtracted from each measurement.

Test No.	**Description**	$I_{\min}$ **(A)**	$I_{\max}$ **(A)**	Observation
1	40 000 µs step delay			No noticeable steps missed
2	20 000 µs step delay	0.669	0.961	No noticeable steps missed
3	10 000 µs step delay	0.559	-	Small slip near calibration start
4	5000 µs step delay	0.252	-	Large number of steps missed
5	2/3 current; 1 hour	0.712	0.713	Minimal system change across the hour
6	3/3 current; 1 hour	2.031	2.261	Stablised current but very hot mount

Table 6.2: Motor Drive Operating Tests @ 12 V supply

Since the boost converter operates as a DC transformer, the current consumed by the motor drive can at maximum current near the start of the hour can be calculated as $2.031 \times \frac{12}{24} \div 2 = 0.509\,\mathrm{A}$. It should be noted, however, that a reference current of 450 mA was designed for, meaning the L6219 is disipپating at least 600 mW. However, since the system is stable near the end of the hour, and the L6219 has thermal shutdown, the system is considered to be within a safe operating region, even though it is clear the power disipپated in the IC increased over the hour.

6.2 PocketQube Unit PCB

Unfortunately, it was decided that a balloon satellite would not be flown by the department. Therefore, integration with the other PocketQube modules was not prioritised for the PCB and the RS-485 line drivers were left off the board. Current consumption for the rest of the components, however, was measured at 31 mA when the system was directly powered from a power supply running at 3.3 V. This is slightly lower than 6 mA lower than the maximum current expected from the GPS and MCU ICs, indicating conformance to the original design.

6.3 Ground Station Antenna

The ground station antenna's return loss was measured using a network analyser to ensure it was correctly matched to 50 ohm. The resultant graph is shown in Figure 6.1. The figure shows the simple matching strip design is effective and was implemented correctly, however it should be noted that the null is not as deep as simulated (only around -10 dB minimum around 427 MHz as opposed to the -50 dB simulated results at the centre frequency of 433 MHz).

There are several reasons why the null may not be as deep as simulated. Firstly, the aluminium foil used is far from an ideal PEC. Secondly, the imperfections in the antenna's construction (e.g. bends in the wire, the PVC and wooden dielectrics that were not simulated,

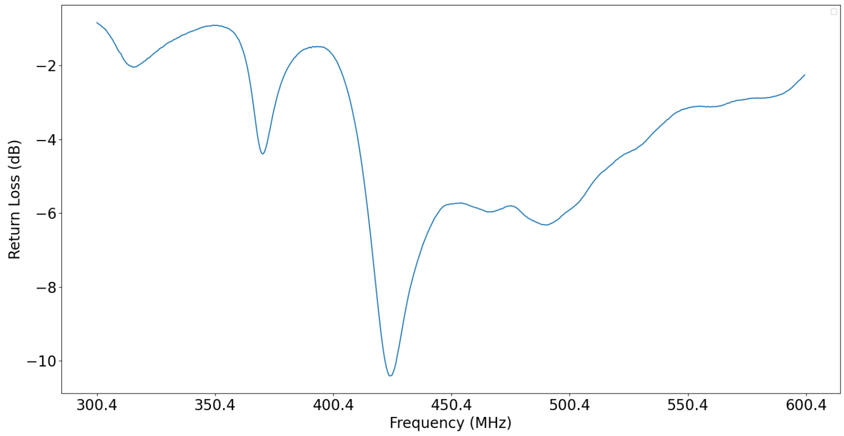

Figure 6.1: Helical Antenna Return Loss vs Frequency

etc.) may cause the match to be non-ideal. Finally, although a short length matching strip performed well in simulations, it is hypothesized that a longer strip might have made the implementation more achieveable due to increased capacitive coupling. Instead of optimizing the antenna build, however, it was decided to run further tests with this system, since the link budget allows for up to a 1 dB matching loss. Optimization is therefore left for future projects. Lastly, the antenna gain pattern unfortunately could not be measured, as a chamber was not available that catered for the low frequency of the system.

6.4 PocketQube Unit Antenna

The return loss of the PQ dipole antenna is shown in Figure 6.2. It is clear that, due to the antenna's simple construction, the resulting match is near-perfect. Since frequencys from around 420 to 440 MHz provide less than 0.1 dB mismatch loss, the final system frequency will be determined by the helical antenna only.

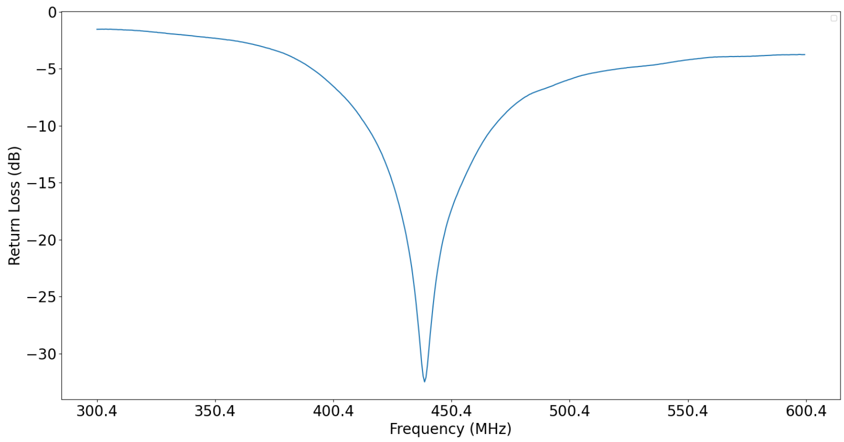

Figure 6.2: Dipole Antenna Return Loss vs Frequency

6.5 RF Module

6.5.1 Setup

The radio module and communication link was initially tested/characterised using two small, off-the-shelf helical antennas, before testing the custom-built antennas. The helical antennas managed an initial range of around 50 m in an urban area with a LoRa spreading factor of 8. This was tested with the one antenna near a window indoors, and the second antenna inside a car. This test served merely as a ”proof-of-concept”, and was not intended as an indication of system performance.

6.5.2 Transmit Power Consumption

The custom-built antennas were then connected to both the PQ and the GS and more detailed tests were conducted. The first test measured the power consumption for the PQ unit as a function of transmit power. This is displayed in Figure 6.3, after subtracting a 31 mA ”no-transmit” current. The maximum current is around 96 mA for the maxium output power (quoted by the RA-02 as 18 dBm +- 1 dBm).

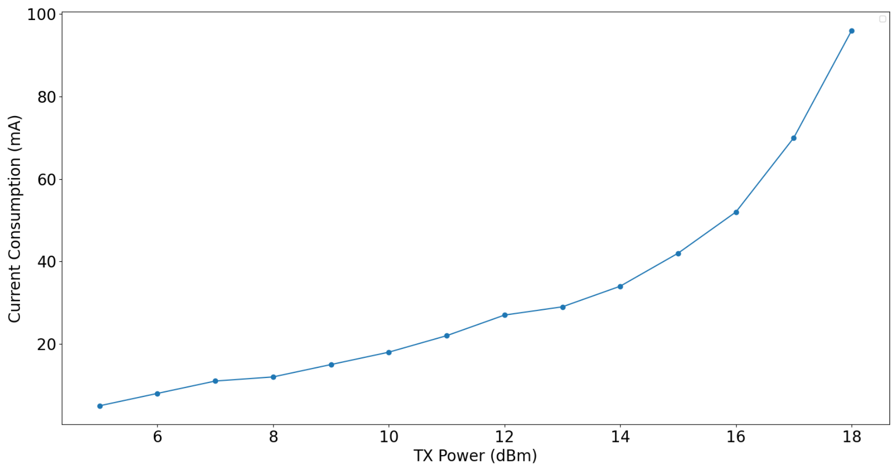

Figure 6.3: TX Output Power vs Current Consumption

6.5.3 Data Rate

To test the possible bit rates as a function of LoRa spreading factor (SF), two RA-02 modules were setup with the same parameters and the bit rate was measured as the SF value was varied. A payload length of 255 was used, with 4/6 CRC, an 8 bit premable, 500 kHz bandwidth, and a 10 ms delay between packets. The bit rate was then measured on the receiving side and is shown in Table 6.3.

Spreading Factor	Theoretical Bit Rate (bps)	Measured Bit Rate (bps)
7	18229	17200
8	10417	10240
9	5859	5800
10	3255	3320
11	1790	1846

Table 6.3

The results show that the system is setup correctly, and that a spreading factor of 8 is the correct choice to achieve the 9600 baud rate requirement.

6.6 Serial Protocol

Basic serial protocol tests still to be added, however the serial commands are currently working properly

6.7 Range

Line-of-sight range tests were conducted by manually positioning both antennas to determine the system's capabilities. Various measurements were done at the originally designed parameters (e.g. SF 8, CR 4/6, 500 kHz) and with automatic gain control (AGC) and the resulting *received signal strength indicator* (RSSI), signal-to-noise (SNR) ratio, and packet reception rate (PRR i.e. percentage of non-corrupted packets received) was recorded. For the unfamiliar reader, the highest (best) theoretical RSSI is 0 dB, and the minimum SNR for SF 8 is -10 dB (LoRa is capable of demodulating negative signal to noise ratios).

Test No.	Range	GS Location	PQ Location	Comments
1	1.4 km	Firgrove Way	M3 Bridge	
2	4.6 km	Constantia	Silvermine	Cloudy conditions
3	9.7 km	Boys' Drive	Simon's Town	
4	34.5 km	Steenbras	Simon's Town	
5	49 km	Takara Stellenbosch	Silvermine	Optimal transmitter placement uncertainty

Table 6.4: Range Test Locations

Tests were done in locations around the Western Cape. These locations are mapped in Appendix E.1 and their descriptions are listed in Table 6.4. The first primitive test (which is not displayed in the Appendix) was a 350 m test on Coetzenburg field. It should be noted, however, that the performance of this test was found to be low compared to subsequent tests. It is assumed that ground bounce was the major contributing factor to this, due to the low operating frequency of the system (around 430 MHz).

The final results plotted as a function of frequency are found in Figures 6.4 and 6.5, with a logarithmic curve fit. All measurements were taken as an average of at least 10 consecutive samples. The dipole was both horizontally and vertically placed. The packet contents were verified using a packet ID, as well as the GPS location of the transmitter.

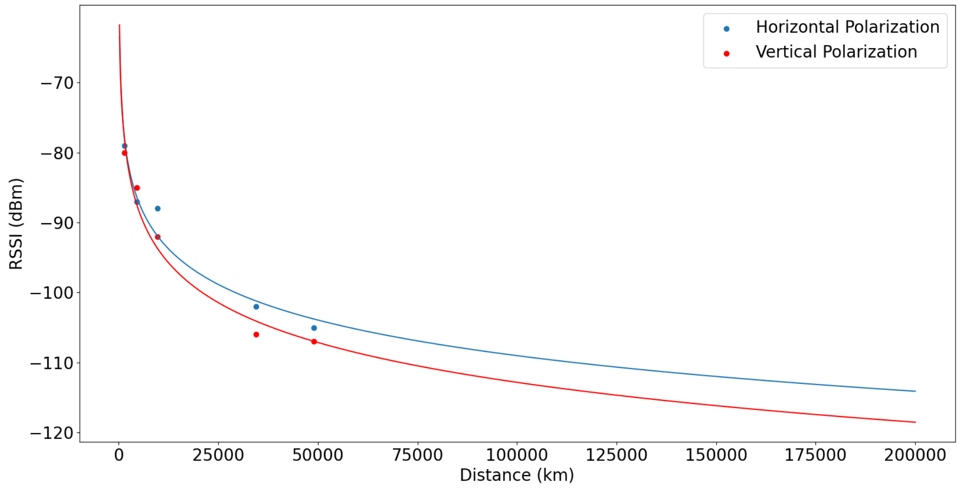

Figure 6.4: Measured RSSI vs Distance

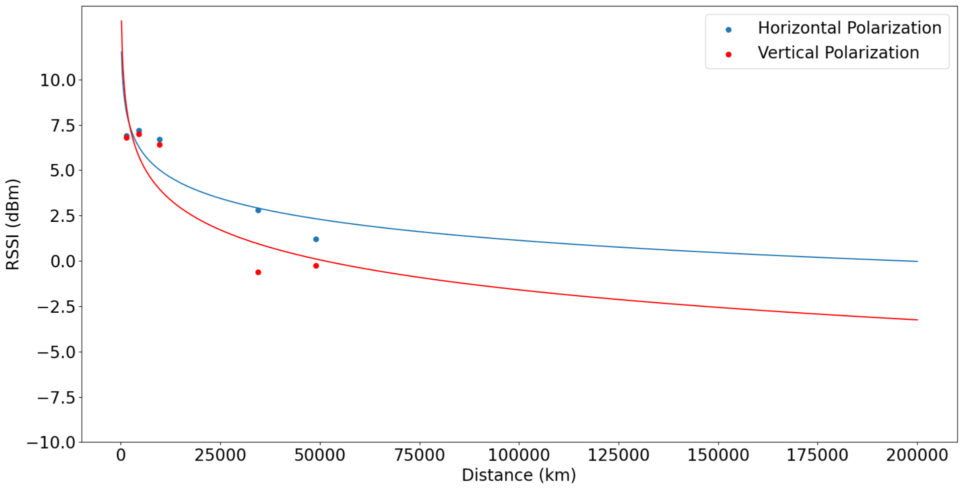

Figure 6.5: Measured SNR vs Distance

The data shows that the system would successfully meet the 110 km range requirement. No CRC errors were found once the system was in steady state for all tests up to the final 50 km test, which recorded an RSSI of around -107 dBm for the vertically polarized case. The predicted RSSI for vertical polarization at 125 km is around -114 dBm, whereas the receiver sensitivty is as low as -119 dBm. It should be noted that the SNR logarithmic fit is not considered reliable, since the receiver appearst to keep the SNR around 7.5 dB for closer distances. However, the RSSI appears to follow a logarithmic curve as predicted by free space path loss formulae. I hope to still do a final 110 km range test from table mountain up the west coast to fully verify my design

6.8 Tracking

6.8.1 Open-Loop

In order to test the GPS pointing and open-loop tracking, a map was printed with lines pointing to locations in the area from a pre-determined location. The ground station was then placed on top of the map at this location, and positioned to face magnetic north using a compass. This test had multiple goals: the mount transfer function, the GPS co-ordinate pointing, and the flight path data following, were all tested simultaneously. An image of the test setup is shown in Figure 6.6.

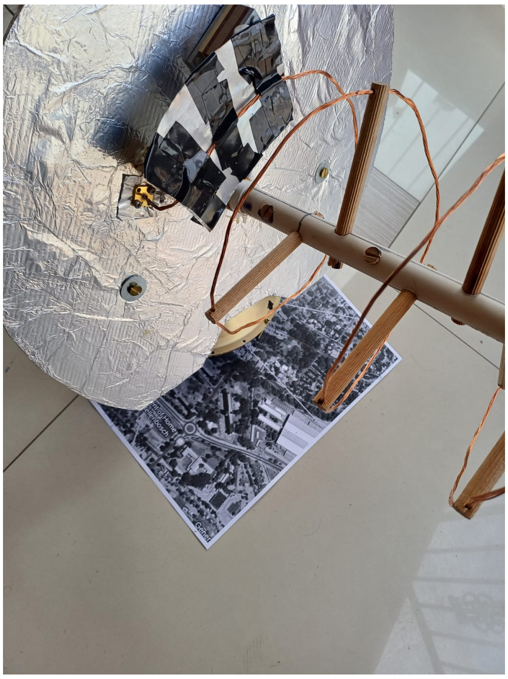

Figure 6.6: Pointing Test Setup

Flight path data containing the pre-determined co-ordinates was then uploaded to the system, and the azimuthal angle was qualitatively confirmed to point in the directions labeled on the map. Further, the elevation angle was measured using a protractor and compared against the expected angle. The system was found to successfully point towards the commanded locations at the desired times. The elevation angle measured were found to be within 5° of the expected angle. This is considered to be within the limitations of the measurements, as the setup to measure the incline of the ground plane was non-ideal.

6.8.2 Closed-Loop

The closed-loop recieved location GPS tracking was tested on an open field at aroudn 300 m range. The PQ unit was carried around the field transmitting its GPS location, and the RSSI was recorded, as well as the pointing direction qualitatively noted.

Figure 6.7: GPS Tracking Locations and RSSI Values

The system was observed to successfully track the transmitter around the entire field without noticeable delay, until it reached a distance of around 10 m, where the pointing direction became unpredictable. This is attributed to the low accuracy of the GPS modules. Since the system is already known to have the capabilities of pointing at a GPS location (from the open-loop tests) and the time requirement is much lower for the balloon satellite system (which requires a tracking speed on the order of 45 degrees in an hour or two) it is clear the system works as designed.

The above test also acts as a primitive test for GPS accuracy, however. The width of the main path being walked on was 3.2 m wide. The furthest deviation of a received GPS co-ordinate from this path is around 3 m (note that the map image is outdated). Therefore, an upper bound on the GPS's accuracy can be set at 6.2 m. Since the required accuracy for the system was calculated to be on the order of a thousand metres (though low is preferable) this setup is deemed to be acceptable.

6.9 Radiosonde

The helical antenna was setup to receive the radiosonde GFSK signal using the RTL-SDR USB dongle. A resultant ”squelch” signal was observed to be received by the radiosonde in one second intervals, and the frequency domain of this signal is shown in Figure 6.8.

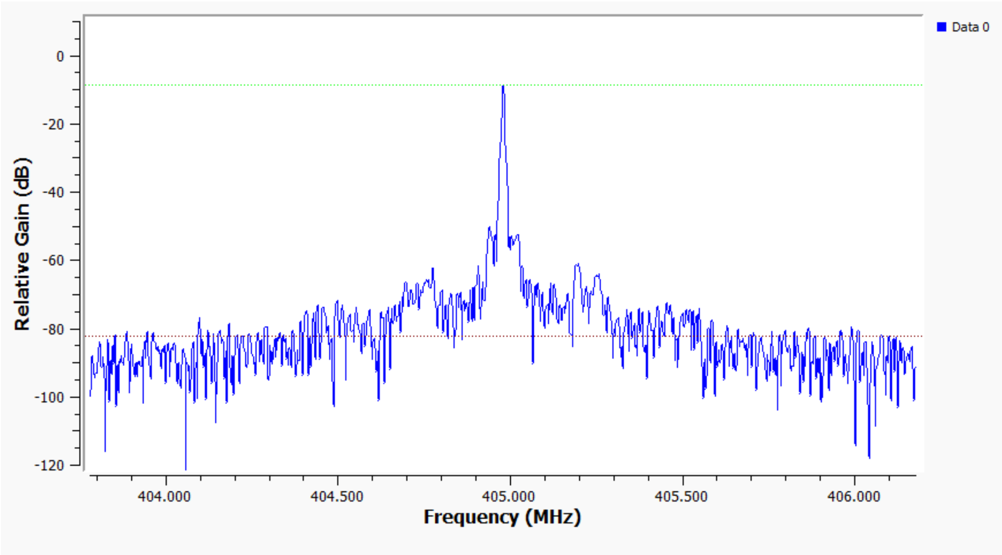

Figure 6.8: Received Radiosonde Signal FFT

Hopefully I can decode this signal to at least get GPS location, otherwise an open-loop test might still be useful?

6.10 Full System

Here I will add any data relating to the final balloon tracking test for my system if it occurs, planned for early next week

7. Conclusion

7.1 Summary

A PocketQube communication system, with a tracking ground station and a PocketQube PCB module, was successfully designed to meet the system requirements for a balloon satellite launch in Saldanha Bay. Unfortunately, the launch did not take place, however several modularized tests helped to prove that the system is fully functional and capable of communicating of the required distances for the course of such a flight.

LoRa proved to be a viable choice for the communication link. Not only did the link meet the throughput requirements, but the increased immunity due to the spread-spectrum technology showed that it is is a priority choice for such sat-com links. The helical antenna design also proved to be effective in the context of the project, as it was easy to manufacture and provided high gain and bandwidth for relatively low effort compared to alternatives.

The open-loop tracking method was successfully implemented, however would need to be tested in a full system run. Closed-loop GPS tracking was shown to work over a short-range, and is claimed to be the prefered method if any sort of link can be estabilished with the satellite. Lastly, the final ground station and PocketQube module design were shown to be effective, and provide a good foundation for future work.

7.2 Future Work

There are various improvements and alternative choices that can be explored in the context of the developed system:

- Improved helical antenna construction. The ground station antenna can be optimized by building it out of more rigid materials, as well as more strict manufacturing procedures, to meet decrease the variance between the simulation and the implementation, and improve the matching and antenna directivity.

- The antenna for the PocketQube was not designed to be deployable, but the half-dipole was shown to provide an effective proof-of-concept. This can worked on, to ensure the antenna is stowed during take-off, and realised in correct position during flight.

- The radiosonde protocol and integration was not fully explored. It would be very useful to be able to decode this information for future flights as a backup option. Further, a dedicated, more sensitive transceiver than an SDR at the relevant frequency, with an RF switch, could be explored. This would provide the ability to change between the custom and radiosonde protocol in software.

- Faster signal strength tracking could be explored further. Although it was not investigated, as a brute-force scan is generally sufficient to initially find the payload and record its GPS location, the flexibility of tracking the payload using only its RF signal may be beneficial.

Bibliography

[1] D. Slabber, "Pocketcube mechanical interface," [Accessed 16-08-2023].

[2] "Tracking a Weather Balloon; High Altitude Science," https://www.highaltitudescience.com/pages/tracking-a-weather-balloon, [Accessed 13-08-2023].

[3] electronicsforu, "Transmission basics: Designing a dipole antenna," https://www.electronicsforu.com/technology-trends/learn-electronics/transmission-basics-designing-dipole-antenna, 2016, [Accessed 16-08-2023].

[4] C. R. A. Inc, "How to make a 433 mhz yagi antenna design for a long-range?" https://lcantennas.com/433-mhz-yagi-antenna-design-for-a-long-range/, 2022, [Accessed 16-08-2023].

[5] Wikipedia, "Inverted-f antenna," https://en.wikipedia.org/wiki/Inverted-F_antenna, 2023, [Accessed 16-08-2023].

[6] Celestis, "What are the "azimuth" and "elevation" of a satellite?" https://www.celestis.com/resources/faq/what-are-the-azimuth-and-elevation-of-a-satellite/, [Accessed 29-09-2023].

[7] P. J. Bevelacqua, "Antenna theory," https://www.antenna-theory.com/, 2022, [Accessed 16-08-2023].

[8] "Weather Balloons — weather.gov," https://www.weather.gov/bmx/kidscorner_weatherballoons#:~:text=The%20balloon%20flights%20last%20for,20%20miles)%20in%20the%20atmosphere!, [Accessed 12-08-2023].

[9] Intermet, "imet-54," https://intermet.co/wp-content/uploads/iMet-54-403MHz-GPS-Radiosonde-Brochure-V5.5.pdf, [Accessed 13-08-2023].

[10] "A multi frequency deployable antenna system for delfi-pq," https://pure.tudelft.nl/ws/portalfiles/portal/57402203/2019_f_74.pdf, [Accessed 13-08-2023].

[11] "Prediction and Tracking a Balloon — Stratospheric Ballooning Association — stratoballooning.org," https://www.stratoballooning.org/tracking, [Accessed 13-08-2023].

[12] R. Israel, "Mercator's projection," https://personal.math.ubc.ca/~israel/m103/mercator/mercator.html, [Accessed 29-09-2023].

[13] C. A. Balanis, "Antenna theory analysis and design," [Accessed 29-09-2023].

[14] "Helix antennas," https://www.microwaves101.com/encyclopedias/helix-antennas, 2018, [Accessed 16-08-2023].

[15] sgcderek, "Helical antenna calculator," https://sgcderek.github.io/tools/helix-calc.html/, [Accessed 29-09-2023].

[16] "A compact low-profile ring antenna with dual circular polarization and unidirectional radiation for use in rfid readers," :https://ieeexplore.ieee.org/stamp/stamp.jsp?arnumber=8822972, [Accessed 03-09-2023].

[17] LinkedIn, "What are the benefits and drawbacks of using different modulation and coding schemes for satcom?" https://www.linkedin.com/advice/0/what-benefits-drawbacks-using-different-6f#:~:text=The%20most%20common%20digital%20modulation,quadrature%20amplitude%20modulation%20(QAM)., [Accessed 29-09-2023].

[18] ——, "What are the benefits and drawbacks of using different modulation and coding schemes for satcom?" https://www.linkedin.com/advice/0/what-advantages-disadvantages-using-qam-over, [Accessed 29-09-2023].

[19] Semtech, "137 mhz to 1020 mhz low power long range transceiver," https://www.semtech.com/products/wireless-rf/lora-connect/sx1278, [Accessed 23-10-2023].

[20] J. Fernandez, "Link budget calculation," https://github.com/FOSSASystems/FOSSASAT-1/blob/master/FOSSA%20Documents/FOSSASAT-1%20Link%20Budget.pdf, [Accessed 29-09-2023].

[21] M. Arias, "Small satellite link budget calculation," https://www.itu.int/en/ITU-R/space/workshops/2016-small-sat/Documents/Link_budget_uvigo.pdf, [Accessed 05-10-2023].

[22] K. Cheung, "The role of margin in link design and optimization," https://s3vi.ndc.nasa.gov/ssri-kb/static/resources/15-0025_A1b.pdf, [Accessed 23-10-2023].

[23] I. Campbell Scientific, "The link budget and fade margin," https://s.campbellsci.com/documents/us/technical-papers/link-budget.pdf, [Accessed 05-10-2023].

[24] GOMspace, "Cubesat space protocol (csp)," [Accessed 24-10-2023].

[25] L. Engineering, "High torque motor," https://cnctar.hobbycnc.hu/ZOTYK%C3%93/NEMA%2017%20motorom%20adatlapja%204218M-01.pdf, [Accessed 13-08-2023].

[26] Fairchild, "Slotted optical switch," https://media.digikey.com/pdf/Data%20Sheets/Fairchild%20PDFs/H22A1,2,3.pdf, [Accessed 29-09-2023].

[27] STMicroelectronics, "L6219 stepper motor driver," https://www.mantech.co.za/datasheets/products/L6219.pdf, [Accessed 29-09-2023].

[28] J. D. Kraus, "Antennas for all applications," [Accessed 29-09-2023].

[29] Gravitech, "Arduino nano," https://www.arduino.cc/en/uploads/Main/Arduino_Nano-Rev3.2-SCH.pdf, [Accessed 29-09-2023].

[30] Intermet, "imet-3100m," https://intermet.co/wp-content/uploads/iMet-3100M-403MHz-Military-Antenna-Receiver-Brochure-V4.5.pdf, [Accessed 12-08-2023].

[31] A. Devices, "Max2659 gps/gnss low-noise amplifier," https://www.analog.com/media/en/technical-documentation/data-sheets/MAX2659.pdf, [Accessed 18-08-2023].

[32] u blox, "Neo-6," https://content.u-blox.com/sites/default/files/products/documents/NEO-6_DataSheet_%28GPS.G6-HW-09005%29.pdf, [Accessed 18-08-2023].

[33] "Review of tracking methods," :http://www.jstor.com/stable/73457, [Accessed 13-08-2023].

[34] I. Campbell Scientific, "The link budget and fade margin," https://s.campbellsci.com/documents/us/technical-papers/link-budget.pdf, [Accessed 03-09-2023].

[35] "Types of orbits — esa.int," https://www.esa.int/Enabling_Support/Space_Transportation/Types_of_orbits#:~:text=Low%20Earth%20orbit%20(LEO),-A%20low%20Earth&text=It%20is%20normally%20at%20an,very%20far%20above%20Earth's%20surface., [Accessed 12-08-2023].

[36] C. P. SOLUTIONS, "Pcb layers explained: Multilayer boards and stackup rules," https://resources.pcb.cadence.com/blog/2019-pcb-layers-explained-multilayer-boards-and-stackup-rules, [Accessed 18-08-2023].

[37] Proteus, "Pcb via stitching and shielding," https://www.labcenter.com/blog/pcb-stitching-and-shielding/, [Accessed 18-08-2023].

[38] SFUPTOWNMAKER, "Pcb basics," https://learn.sparkfun.com/tutorials/pcb-basics/all, [Accessed 18-08-2023].

[39] A. Devices, "Pcbs layout guidelines for rf and mixed signal," https://www.analog.com/en/technical-articles/pcbs-layout-guidelines-for-rf--mixedsignal.html, [Accessed 18-08-2023].

[40] N. T., “Standard 4- and 6-layer pcb stackups,” https://www.bitweenie.com/listings/standard-4-and-6-layer-pcb-stackups/, [Accessed 18-08-2023].

[41] P. Electronics, “Routing guidelines for rf pcbs,” https://www.proto-electronics.com/blog/routing-guidelines-rf-pcb, [Accessed 29-09-2023].

[42] J. D. Kraus, “Antennas for all applications,” [Accessed 29-09-2023].

A. Project Planning

Still to be formulated into a gantt chart Week 01 (24/07 to 30/07): Problem formulation; requirements gathering Week 02 (31/07 to 06/08): Initial research; component selection Week 03 (07/08 to 13/08): System-level design; initial system layout; components ordered Week 04 (14/08 to 20/08): PCB design without traces; initial circuit design Week 05 (21/08 to 27/08): Component prototyping; Full PCB design; initial antenna design; Week 06 (28/08 to 03/09): Mechanical design; Custom protocol investigation; PCB ordered Week 07 (04/09 to 10/09): (Test week) Week 08 (11/09 to 17/09): Initial build Week 09 (18/09 to 24/09): Software design; initial testing Week 10 (25/09 to 01/10): Software design; debugging Week 11 (02/10 to 08/10): Reporting Week 12 (09/10 to 15/10): Design improvement Week 13 (16/10 to 22/10): Testing Week 14 (23/10 to 29/10): Reporting Week 15 (30/10 to 05/11):

B. Schematics

B.1 Ground Station

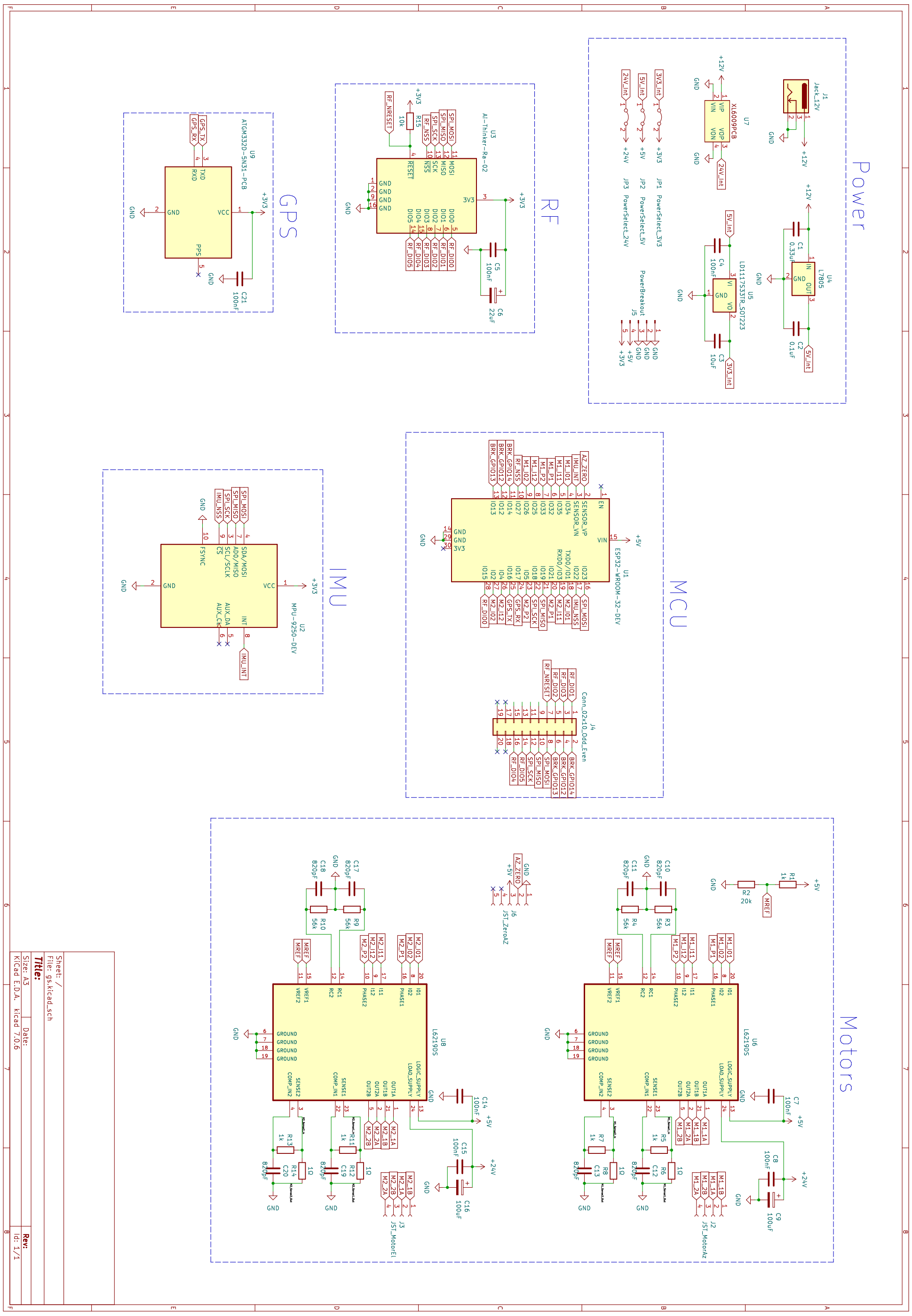

B.2 PocketQube Unit

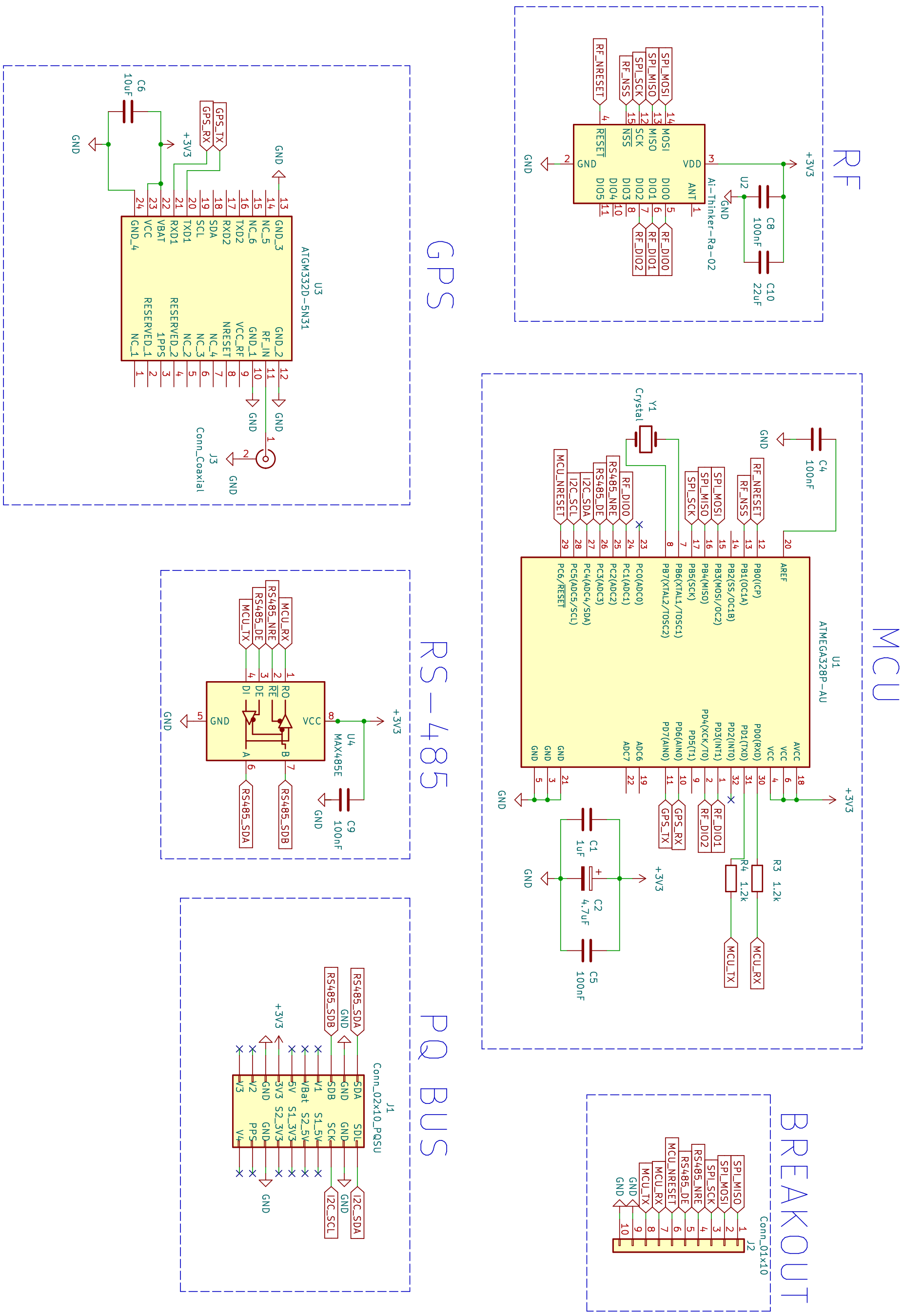

B.3 Errata

- Full errata for PCB designs still to be added

C. Standards

C.1 PQSU

Pocketcube Mechanical Interface

Dirk Slabber, MEng | Electronic Systems Laboratory| Stellenbosch University

13/06/2023

* unless otherwise specified all measurements are to "The PocketQube Standard" [Issue 1, 7th of June, 2018], PQ9 and CS14 standard.

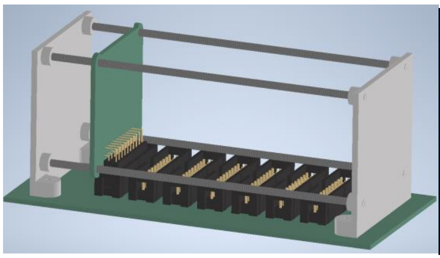

Figure 1- pocketcube structure

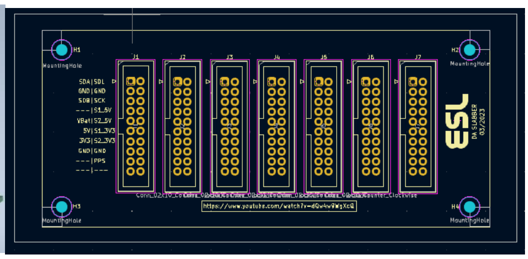

Figure 2- pocketcube bus layout

Physical Envelope

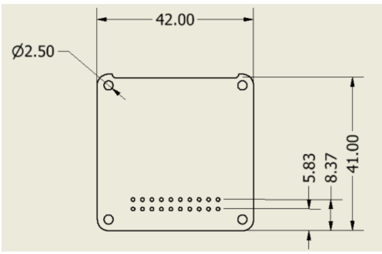

Figure 3-dimensions of the slot

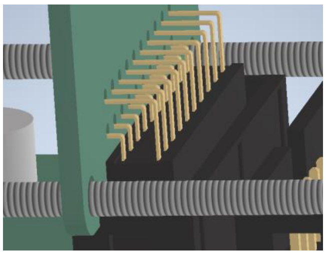

Figure 4-90-degree pins

Please take care to not place components such that it will obstruct the 90-degree bus pins as well as the nuts that will be hold the slot in place around the four mounting holes. Components may project up to 8mm away from the board and still slot in with another board directly next to it.

Electrical Connection

Each slot is has twenty pins connected a bus in the main plate. Pin 1 is located top right on figure 3, pin 11 bottom right and so on. The suggested pinout on the bus is as follows:

1	SDA	SDL	11
2	Ground	Ground	12
3	SDB	System Clock	13
4	User defined	5V Switch 1	14
5	Power source	5V Switch 2	15
6	5V line	3.3V Switch 1	16
7	3.3 line	3.3V Switch 2	17
8	Ground	Ground	18
9	User defined	PPS	19
10	User defined	User defined	20

C.2 SUNCQ

SUNCQ Protocol

Commands

The following lists all commands from TNC to host and vica-versa. The command reservations are:

- 0x00 to 0x2F Host-to-TNC DO commands
- 0x30 to 0x5F Host-to-TNC SET commands
- 0x60 to 0x7F Host-to-TNC GET commands
- 0x80 to 0x9F TNC-to-Host STATUS replies
- 0xA0 to 0xCF TNC-to-Host DATA replies
- 0xD0 to 0xFE Reserved
- 0xFF Invalid

Code	**Name**	**Function**	**Payload**	**Bytes**	**Comments**
0x00	RESET	Reset the system	-	0	
0x01	CALIBRATE	Calibrate the system	-	0	Full calibration e.g. ground station and all sub-systems
0x02	RETURN_TO_START	Return the system to its starting state.	-	0	The starting state is post-calibration.
0x03	RETURN_TO_STOW	Return the system to its stow state.			The stow state is pre-calibration. Typically used before system shutdown
0x30	SET_TNC_MODE	Enter a TNC mode	See *TNC_MODE*	1	
0x31	SET_TRACK_MODE	Set tracking mode	See *TRACK_MODE*	1	
0x32	SET_PATH_DATA	Upload flight path data	CSV file. See *Flight Path Data.*	Any	The payload length is provided as the first 8 bytes.
0x33	SET_POINT_DIRECTION	Set the direction that the mount should point at			Only applicable when no tracking mode is selected
0x60	GET_SIGNAL_RSSI	Get RSSI of the signal	-	0	
0x61	GET_LOCATION	Get location of the ground station	Lat;Lng;Alt (f32;f32;f32)	12	
0x80	TNC_STATUS	Sent by the TNC as an ACK or status alert.	See *STATUS_CODE.*	1	Status 0x00 is used as an "ACK" command.
0x81	TNC_MESSAGE	Sent by the TNC to communicate a String message to the host.	char[]	Any	A newline character terminates the message
0xA0	SIGNAL_RSSI	Response to *GET_SIGNAL_RSSI*	float	4	
0xD0-0xFE	RESERVED	Reserved			Reserved for future use
0XFF	INVALID	Invalid			For internal use

Details

TNC_MODE

Value	Description
0x00	Normal mode
0x01	KISS mode. This mode is exited using the KISS 0xFF command.

TRACK_MODE

The tracking mode is a combination flag i.e. multiple bits can be ORed together to specify that the payload must be tracked using multiple methods at once.

Value	Description
0x00	No tracking. Mount can be moved by setting the pointing vector.
0x01	Use uploaded GPS data
0x02	Use received GPS data (from payload)
0x04	Use signal strength, but only for an initial scan
0x08	Use signal strength, with dynamic conical scanning

STATUS_CODE

The following is a list of status codes that might be sent from the TNC to the host:

Value	Description
0x00	Acknowledge
0x01	Payload tracking unsuccessful/payload lost

Flight path data

Flight path data can be uploaded in the form of a little-endian binary stream (i.e. each field should be least significant byte first). The first field is a 2-byte number indicating the number of flight path instances to follow. Then, the fields below should be provided. Such a file can be generated by predicting a flight path at https://predict.sondehub.org/ , generating a CSV file, and then using the data to generated a binary stream. In the current implementation, only 200 entries are catered for – if longer flights are needed, then multiple streams should be set from the host intermittently. Time should be in Unix time (seconds since Epoch).

Name	Type
Time	uint64
Latitude	float32
Longitude	float32
Altitude	float32

D. Implementations

D.1 Ground Station

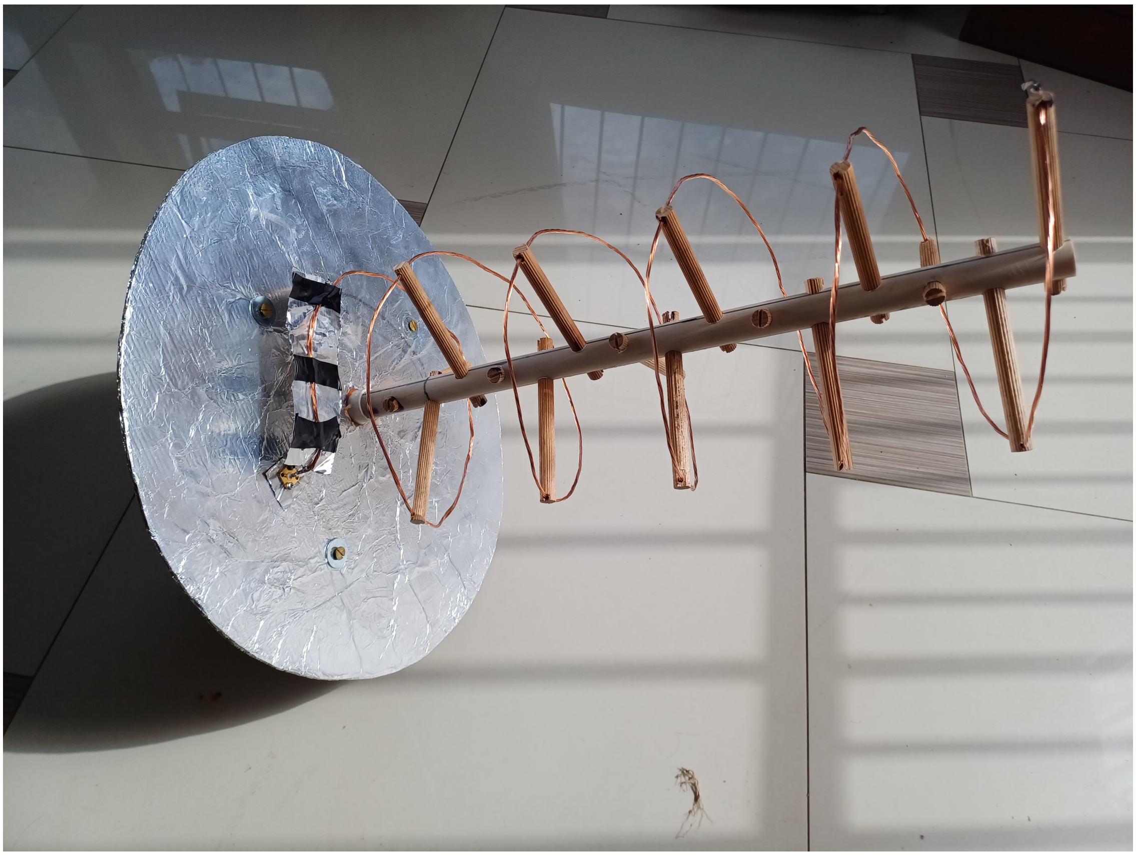

Figure D.1: Ground Station Original Antenna Build

D.2 PocketQube

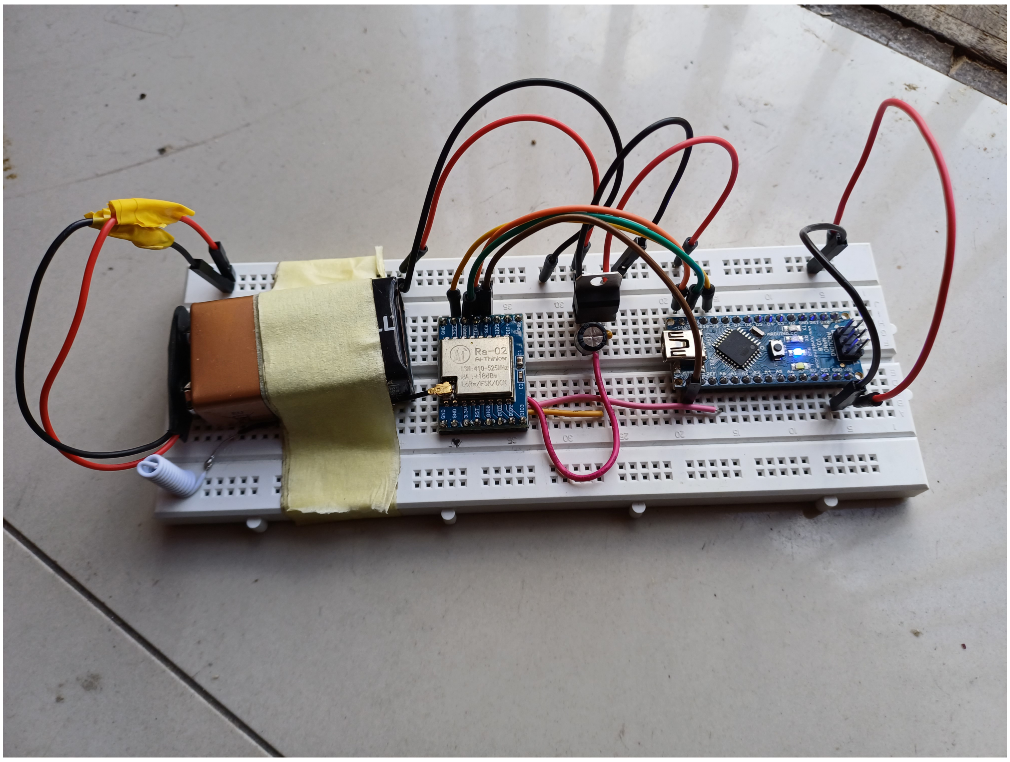

Figure D.2: PocketQube Breadboard for Testing

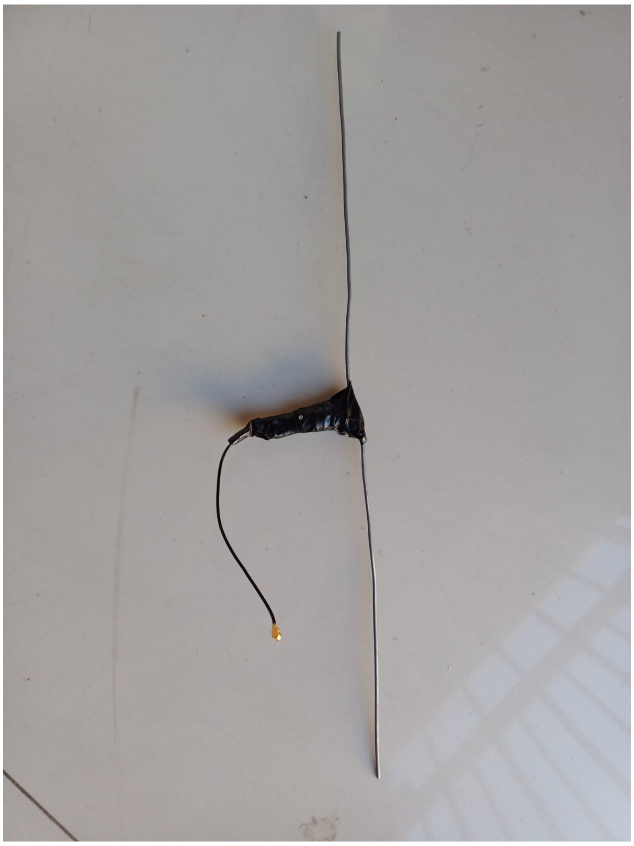

Figure D.3: PocketQube Dipole Antenna

D.3 GUI

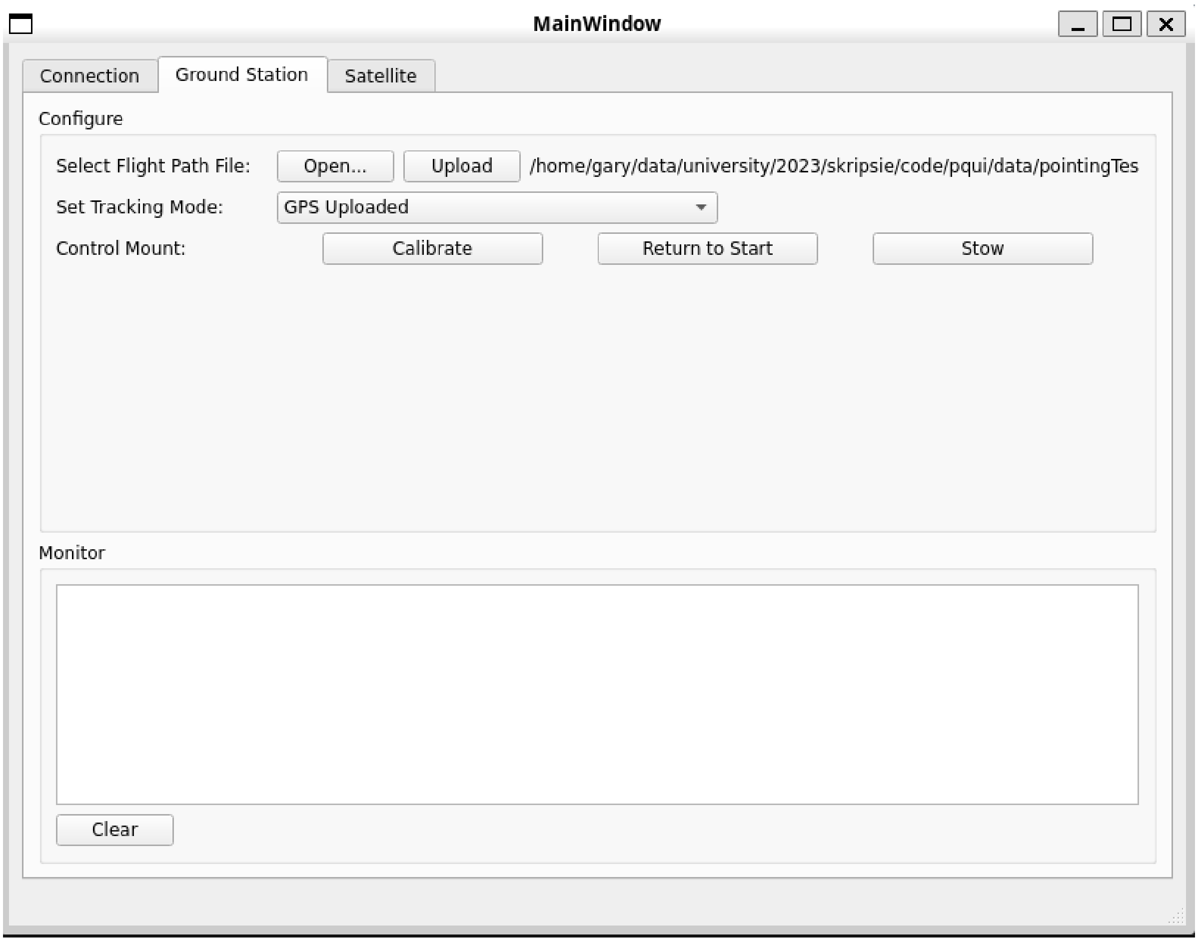

Figure D.4: GUI Snapshot

E. Tests

E.1 Range Tests

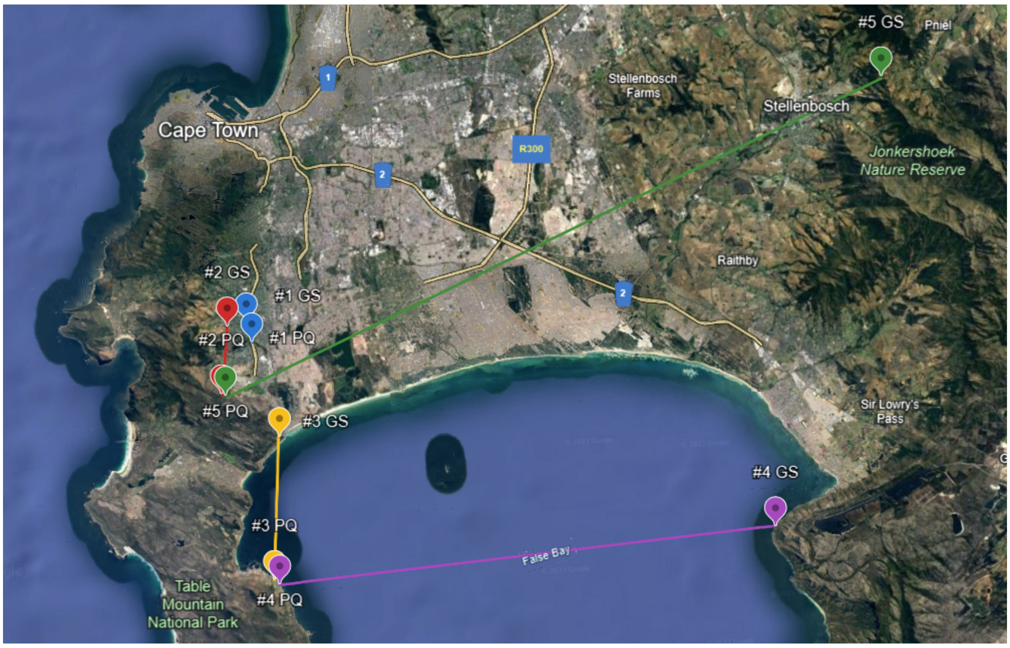

Figure E.1: Range Test Locations